Progress in Polymer Science 99 (2019) 101164

Contents lists available at ScienceDirect

Progress in Polymer Science

journal homepage: www.elsevier.com/locate/ppolysci

Recent advances in stimuli-responsive polymer systems for remotely controlled drug release

Aitang Zhang[a], Kenward Jung[b], Aihua Li[a], Jingquan Liu[a,*], Cyrille Boyer[b,*]

[a] College of Materials Science and Engineering, Institute for Graphene Applied Technology Innovation, Collaborative Innovation Centre for Marine Biomass Fibers, Materials and Textiles of Shandong Province, Qingdao University, Qingdao 266071, China
[b] Centre for Advanced Macromolecular Design (CAMD), Australian Centre for NanoMedicine, School of Chemical Engineering, The University of New South Wales, Sydney, NSW 2052, Australia

ARTICLE INFO

Article history:
Received 21 July 2019
Received in revised form
25 September 2019
Accepted 27 September 2019
Available online 1 October 2019

Keywords:
Stimuli-responsive polymers
Functional materials
Drug delivery
Polymeric nanoparticles
Remote control

ABSTRACT

Promoted by recent advances in developing nanomaterials and drug delivery, stimuli-responsive polymer systems that can remotely trigger drug release in a spatiotemporal manner has attracted significant attention in biotechnology. Implementation of remote-controlled release requires functional polymers to be susceptible to specific physical and/or chemical stimuli. In this minireview, we focus on the recent advances in the construction of stimuli-responsive polymer systems for remotely controlling drug release in response to an externally applied stimulus (light, microwave, magnetic field, electric field and ultrasound). The design of the stimuli-responsive polymer systems and formulations to remotely control the release of drug molecules is also highlighted in this minireview. Furthermore, the potential in biomedical applications and the perspectives of future developments of these stimuli-responsive polymer systems are also briefly discussed.

Abbreviation: 3-IC, 3-indenecarboxylic acid; AMF, alternating magnetic field; ANBB, 2-(4'-N-dimethylamino-4-nitro-[1,1'-biphenyl]-3-yl(butane-1,4-diyl dicarbonyl; ATRP, atom transfer radical polymerization; AuNPs, goldnanoparticles; BCP, block copolymer polymersomes; [14C]-sucrose, radiolabelled sucrose; CB[8], cucurbit[8]; β-CD, β-cyclodextrin; Ce6, chlorine e6; CP, chitosan-g-polyaniline; CT-26, CD44 receptor negative cells; DAPI, 4',6-diamidino-2-phenylindole; DASA, donor-acceptor Stenhouse adducts; DNPs, doxorubicin nanoparticles; DNQ, 2-diazo-1,2-naphthoquinone; DOX, doxorubicin; DPPC, 1,2-dipalmitoyl-sn-glycero-3-phosphocholine; DSPE-PEG2000, 1,2-distearoyl-sn-glycero-3-phosphoethanolamine-N-methoxy(polyethylene glycol)-2000; EFGP, enhanced green fluorescent protein; ETX, ethosuximide; F127, poly(ethylene oxide)-poly(propylene oxide)-poly(ethylene oxide); FA, folic acid; FCNPs, Fluorescentcarbon nanoparticles; Fc, ferrocene; FDA, US Food and Drug Administration; FTMA, (11-ferrocenylundecyl) trimethylammonium bromide; GPC, gel permeation chromatography; IONPs, ironoxide nanoparticles; ITO, indium tin oxide; IVO24, a peptide; LCST, lower critical solution temperature; LSMO, lanthanum strontium manganese oxide; MC, merocyanine; MCF-7, breast cancer cells; MCF-7/ADR, MCF-7 cells with addition of DOX; MCF-7/MDR, multidrug resistant MCF-7 subline; MDA-MB-231, CD44 receptor over expressed human breast cells; MRI, magnetic resonance imaging; mRPC, mouse retinal progenitor cells; MWNT, multiwalled carbon nanotube; NGF, nerve growth factor; NSET, nanomaterial surface energy transfer; 1O2, singlet oxygen; OD, oxidized dextran; PAA, poly(acrylic acid); PAAm, poly(acrylamide); PAEA, 2-hydroxyethyl acrylate; PAH, poly(allylamine hydrochloride); PAN, poly(acrylonitrile); PAPNBMA, poly(5-(3-(amino)propoxy)-2-nitrobenzyl methacrylate); PBMA, poly(butyl methacrylate); PCL, poly(caprolactone); PDA, poly(dopamine); PDMAEMA, poly(dimethylaminoethyl methacrylate); PDT, photodynamic therapy; PEG, poly(ethylene glycol); PEO, poly(ethylene oxide); PG, 1-palmitoyl-2-oleoyl-sn-glycero-3-phospho-rac-glycerol; PHBPI, poly(phenyl isocyanide); PHPPI, poly(L-hydrophilic phenyl isocyanide monomer); PLDL, poly(D, L-lactic acid); pLINFU, pulsed low intensity non focused ultrasounds; PLGA, poly(D,L-lactic-co-glycolic acid); PMAA, poly(methacrylic acid); PMMA, poly(methyl methacrylate); PNAGA, poly(N-acryloylglycinamide); PNAm, poly(N-acryloylglycinamide); PNBOC, poly(2-nitrobenzyloxycarbonylaminoethyl methacrylate); PNIPAM, poly(N-isopropylacrylamide); PNIPMAM, poly(N-isopropylmethacrylamide); PpPD, poly(p-phenylenendimine); PPO, poly(propylene oxide); PPV-ST, poly(p-phenylene vinylene) functionalized donor-acceptor Stenhouse adducts and folic acid units; PPy, poly(pyrrole); PRF, pulse repetition frequency; PS, poly(styrene); P(S-BMA), poly(styrene-stat-butyl methacrylate); PTPEPI, poly(tetraphenylethene-functionalized-phenyl isocyanide); PTTAMA, poly(2-((((5-methyl-2-(2,4,6-trimethoxyphenyl)-1,3-dioxan-5-yl)methoxy)carbonyl)amino)ethyl methacrylate); PTX, paclitaxel; PVA, polyvinyl alcohol; RF, radio-frequency; rGO, reduced graphene oxide; ROS, reactive oxygen species; SAR, specific absorption rate; siRNA, small interfering RNA; SP, spiropyran; SPA, spiropyran-based monomer containing a carbamate linkage; Tc, Curie temperature; TEM, transmission electron microscope; *Tg*, the glass transition temperature; TS/A, breast cancer cells; VA, vinylacetic acid; VA-060, 2,2'-azobis[2-[1-(2-hydroxyethyl)-2-imidazolin-2-yl]propane] dihydrochloride.

* Corresponding authors.
E-mail addresses: jliu@qdu.edu.cn (J. Liu), cboyer@unsw.edu.au (C. Boyer).

https://doi.org/10.1016/j.progpolymsci.2019.101164
0079-6700/

Contents

1. Introduction

Great effort has been devoted to the discovery and development of new therapeutic drugs for the treatment of severe diseases every year [1–3]. However, the efficacy of these drugs are often diminished by nonspecific biodistribution and/or rapid clearance from the body [4]. Moreover, many therapeutic agents often present limitations such as poor water solubility and low cellular uptake [5–7]. Drug delivery and release systems aim to solve these deficiencies and have therefore received tremendous attention [8–12]. Rapid and ongoing developments in the field of nanotechnology have been translated into a broad range of nanostructured drug carriers of diverse size, architecture and surface properties [13,14], such as liposomes [15], polymer micelles [16], nanocapsules [17], dendrimers [18] and hybrid nanoparticles [7,19] made of iron oxide [7], silica [20,21], gold [22,23] or metal sulfide frameworks [24,25]. The role of these nanocarriers is to maintain drug concentrations within a narrow therapeutic window to avoid both high cytotoxicity (overdose) and ineffective treatment (under-dosing) [18,26]. As inert vehicles, these nanocarriers ideally possess excellent biocompatibility, high drug loading efficiency and effective cellular uptake [15,27–31]. Polymer chemists have access to a rich library of functionalization chemistries to impart these desirable qualities [32].

Despite the considerable advances in drug delivery technologies made over the past few decades, most examples have been limited to monotonic drug release profiles which do not take into account the specific needs of the patient nor the changes in physiology that occur during treatment [33–35]. More sophisticated drug delivery systems are increasingly explored in an attempt to address the problems of multidrug resistance, severe side effects and metastasis [36]. An ideal delivery system should be able to control the release of drugs in respect to dosage, duration, location and even the timing. This advanced approach to drug delivery can be facilitated by the design of functional polymers which recognize their microenvironment and respond in a manner akin to living organisms [4,37,38]. Alternatively, polymer systems responding to noninvasive external stimuli may be utilized to afford on demand triggering of drug release by an operator [39–43]. These latter remotely-triggerable polymer systems enable targeted and reliable tuning of drug release that is controlled by an operator and is a step towards more personalized therapeutic protocols [44–47].

In this minireview, we focus on remotely controlled trigger systems in which the drug is released on-demand from the specifically designed nanocarriers exhibiting stimuli-responsiveness to light, microwave, magnetic or electric fields and ultrasound (Scheme 1). More attention is paid to the drug delivery systems, which have received intense interest in the past few years because of their unique and broad applicability for remotely controlled drug release with enhanced therapeutic effectiveness and/or reduced systemic toxicity. This minireview concludes with a discussion on the future perspectives regarding novel multi-modal stimuli-responsive drug delivery systems and their potential biomedical applications.

2. Stimuli-responsive polymer systems and biomedical applications for triggered drug release

2.1. Light responsive systems

Stimuli-responsive polymer systems have proven to be the efficient tools to achieve controlled drug release which improves the therapeutic effects and reduces the side effects [15,48–51]. In the past few years, various nanomaterials that respond to varying internal (including pH, redox potential, various ions, biomacromolecules, enzymes, glucose or specific analytes) or external (including temperature changes, light, microwave, magnetic field, electric field and ultrasound) stimuli have been widely designed and explored for drug delivery [26,52–55]. Although functional polymers which respond to internal stimuli can be advantageous in their ability to facilitate drug release according to their specific biological microenvironment, so far they have demonstrated limited control over the rate of release [56–58]. In contrast, delivery systems which can be triggered by external stimuli have the advantages of superior spatiotemporal control over the drug release. Due to its advantages over other external stimuli, light has been established as an attractive stimulus for constructing responsive drug delivery systems [59,60]. A large variety of photo-responsive systems activatable by a specific wavelength have been developed and reported in the past few years to achieve on-demand drug release; their advantages arise from the non-invasiveness of light and the possibility of remote spatiotemporal control [4,61,62]. Nanocarriers capable of undergoing physical or chemical changes in response to light irradiation are attractive for designing safe treatment regimens that offer spatiotemporal control over the release of encapsulated therapeutic payloads (Table 1).

2.1.1. Near-infrared light responsive systems

Conventional light-induced drug delivery is only applicable to the organs of body that can be directly illuminated such as the skin. However, it is possible to replace conventional light sources with NIR light (700 nm–1100 nm). This has enormous advantages for triggering drug release as it enables precise and controlled release of the payload at the target site in a non-invasive manner [63]. Typically, compared to visible and UV sources, NIR light possesses superior biocompatibility and undergoes less scattering and absorption, affording enhanced penetration while causing less harm to skin/tissue [64]. NIR light can be transformed into heat with the assistance of various photothermal materials [65,67]. With these advantages in mind, developing various novel systems based on NIR light to remotely control drug delivery and release is highly attractive for biomedical applications [4,11,17,66,67].

Table 1
Summary of light triggered drug release *in vivo*/*vitro*.

Ref. Year	Irradiation protocol	Light-responsive system	Light-responsive release mechanism	Therapeutic agents and dose
[68] 2018	NIR 808 nm 10 W 240 min UV 365 nm 40 mW cm^{-2} 70 min	PEG-PDMAEMA@ 2-diazo-1,2-napthoquinone	Hydrophobic to hydrophilic isomerization *via* the Wolff rearrangement	Coumarin 102 1.5 wt%
[69] 2018	NIR 808 nm 5 min 0.2/0.5/0.8/1.0/2.0 W cm^{-2}	PPy coated PCL-PTX	Induced hyperthermia enhanced the permeability	Paclitaxel 1.5 wt%
[70] 2018	NIR 808 nm 4.0 W cm^{-2} 5 min	PEG-*b*-P(NAGA-*co*-AN) micelles	Micelles disassembled under the induced hyperthermia	Doxorubicin/ 1.5 mg/mL
[66] 2018	NIR 808 nm 1 W cm^{-2} 10 min	Maleimide functionalized PDPP-DBT nanoparticles	Heat-inducible promoter by photothermal-responsive polymer	EGFP gene 20 μg mL^{-1}
[71] 2018	NIR 808 nm 2 W cm^{-2} 10 min	PNAm-PDAAu-DOX hydrogel	Lighted triggered reversible gel-sol transition	Doxorubicin 20 mg kg^{-1}
[72] 2018	NIR 808 nm 5 W cm^{-2} 5 min	DNPs/NH_4HCO_3@ PDA	PDA films broken by the gases induced from the decomposition of NH_4HCO_3	Doxorubicin 3 mg kg^{-1}
[73] 2013	NIR 765/808/980 nm 400/800/1200 mW 30 min	*N*-succinyl-*N*′-4-(2-nitrobenzyloxy)-succinyl-chitosan micelles	Bond-breaking occurring from the absorption of light	Cypate fluorescein 29.2 wt%
[74] 2014	NIR 808 nm 1.5 W cm^{-2} 5 min	Poly(NIPAM-AAm)- fluorescent carbon nanoparticles hybrid nanogels	Reversible swelling/shrinking transition	Curcumin 1 mg/mL
[76] 2018	NIR 808 nm 6 min 200 mW cm^{-2}	PEO-*b*-PFMA core-cross-linked micelles	Induced reactive oxygen species by light can cleave diselenide bonds in the core of micelles	Doxorubicin 10 mg/mL Indocyanine green 1.8 mg/mL
[77] 2015	NIR 650-700 nm 24 mW cm^{-2} 2 min	Pluronic copolymer P123@DOX/cypate@PEG-*b*-PDPA	Induced the hyperthermia effect	Doxorubicin 8 μg mL^{-1}
[78] 2015	Vis 530 nm 1 mW cm^{-2} 15 min UV 365 nm 1.5 mW cm^{-2} 2 min	Poly(ethylene oxide)-*b*-poly(spiropyran) polymersomes	Reversible phototriggered isomerization (hydrophobic spiropyran and zwitterionic merocyanine)	2'-deoxy-5-fluorouridin/ 4′,6-diamidino-2-phenylindole/ Doxorubicin 2 mg mL^{-1}
[79] 2018	Vis 430 nm 230 mW cm^{-2} 30 min	PEO-*b*-PCSSMA polymersomes	Inter/intrachain amidation reactions induced by light	Doxorubicin 10 mg/mL
[80] 2018	Vis 488 nm 10 mW cm^{-2} 0-6 min	Poly(p-phenylene vinylene)/donor-acceptor Stenhouse adduct/folic acid	Hydrophobic to hydrophilic isomerization	Camptothecin/Doxorubicin/ Cyanine5 10 wt% of the total polymer content
[81] 2014	Vis 420 nm/UV 365 nm 30 min	Poly(*N*,*N*-dimethylacrylamide)-*b*-poly(benzyl carbamate)	Polymersomes disintegrated into water-soluble molecules and hydrophilic blocks under light	Camptothecin Doxorubicin 1 mg/mL
[82] 2015	Vis 400-500 nm 0.18 W 0.21 mW cm^{-2} 40 min	2-(40-*N*-dimethylamino-4-nitro-[1,10-biphenyl]-3-yl)butane-1,4-diyl dicarbonyl	Photoexpansile swelling by blue visible light	Dexamethasone IR780 1% wt% of the total polymer content
[83] 2017	Vis 420∼530 nm 10 mWcm^{-2} UV 365 nm 10 min	PEG-based hydrogels/ nitrobenzyl moieties	Bond-breaking occurring from the absorption of light	Mesenchymal stem cells/ L929 murine fibroblast cells
[84] 2015	Vis 660 nm 50 mW cm^{-2} 10 min	$^1O_2$-PEG-*b*-PCL	Singlet oxygen-medicated photocleavage under visible light	Photosensitizer/Ce6/ Doxorubicin 0.3 μg mL^{-1}
[85] 2018	Vis 532/632 nm 100 mW cm^{-2} 5 min	PVA/PEI/chitosan/ IONPs	Photooxidation action medicated payload release	Rose Bengal 20 μM
[87] 2014	UV 365 nm 1.2 W cm^{-2} 0-20 min	Poly(ethylene oxide)-*b*-poly(2-nitrobenzyloxycarbonylaminoethyl methacrylate)	Hydrophobicity to hydrophilicity transition and membrane permeabilization	Doxorubicin Nile red 1.8 mg/mL
[88] 2018	UV 365 nm 200 W 48 hours	Poly(ε-caprolactone)-*b*-poly(methacrylic acid-*co*-spiropyran methacrylate)	Hydrophobic spiropyran isomerized to hydrophilic merocyanine (H^+)	Doxorubicin 0.4 mg/mL
[89] 2018	UV 365 nm 10 min 0.1 mW cm^{-2}	PEG-*star*-2-(4-nitro-3-benzyl carbonate camptothecin) phenoxyethyl methacrylate	*o*-nitrobenzyl linker cleavage triggered by UV light	Camptothecin 17.4 mg/mL
[90] 2018	UV 365 nm 3 hours	PNBOC-PTPEPI-PHPPI	Hydrophobic PNBOC to hydrophilic PAEMA	Camptothecin Nile red 1 mg/mL
[91] 2017	UV 365 nm 15 mW cm^{-2} 0-3 min	Poly(acrylic acid-*co*-spiropyran methacrylate) nanogel	Hydrophobic spiropyran isomerized to hydrophilic merocyanine	Doxorubicin 2 mg/mL
[92] 2015	UV 365 nm 20 mW cm^{-2} 0-20 min	Poly(*N*-isopropyl acrylamide-*co*-spiropyran)	Hydrophobic to hydrophilic isomerization	Coumarin 102 0.1 mg/mL
[93] 2018	UV 365 nm 0.34 mW cm^{-2} 0∼20 min 8 W	Giant supramolecular vesicles of cucurbit(8) uril (CB(8))	Trans to cis isomerization of 3,4,5-tris(n-dodecyloxy)benzoylamide-azobenzene	Doxorubicin 1.5 μg/mL
[95] 2017	UV 365 nm $P < 0.05$ 10 min	mPEG-*b*-poly(5-(30amino-propoxy)-2nitrobenzyl methacrylate)	Charge-reversal in response to photostimulus	siRNA 16 μg/mL
[96] 2017	UV 2.8 W cm^{-2} 450 W 20 min	Poly(ethyl glyoxylate)/poly(ethylene oxide)	Cleavage of the linker end-caps triggered by UV light	Doxorubicin/ Curcumin 13 wt%
[98] 2015	UV 350 nm 195 min	Light-sensitive degradable polymer based quinone-methide	Cleavage of triggering group by light induces cyclization	Nile red 19 μg/mL
[99] 2014	UV 254 nm 100 W 30 min	Hyperbranched polyglycerols based spiropyran	Photoisomerization of hydrophobic spiropyran to hydrophilic merocyanine	Pyrene 5.2 mg/L

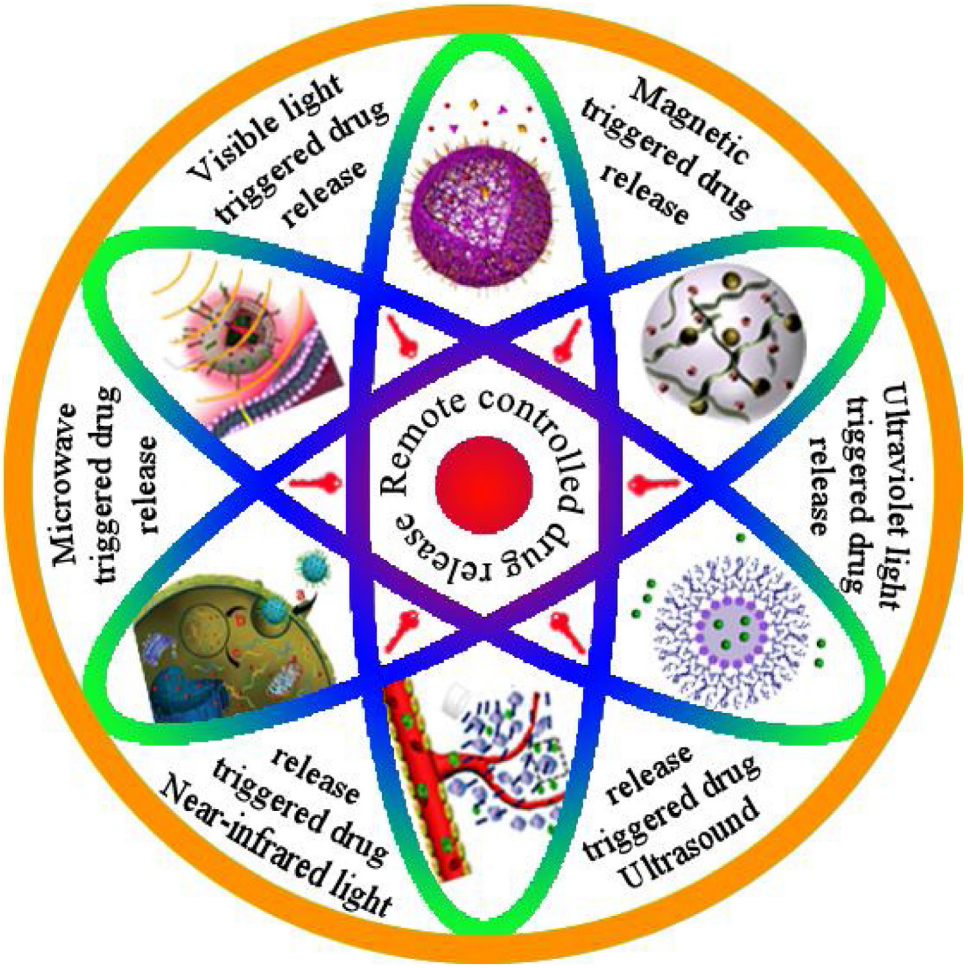

Scheme 1. Schematic illustration of stimuli-responsive polymer systems applied for remotely controlled drug release.

Wang and co-workers recently reported a novel pH and light sensitive drug delivery system based on 2-diazo-1,2-naphthoquinone (DNQ). The key part of this work was the incorporation of hydrophobic DNQ moieties which could undergo transformation into hydrophilic 3-indenecarboxylic acid (3-IC) functionalities *via* either a one-photon (UV) or two-photon (NIR, 808 nm)-induced Wolff arrangement. The DNQ moieties were incorporated through a quarternization reaction of the tertiary amines contained in the amphiphilic poly(ethylene glycol)-*b*-poly(dimethylaminoethyl methacrylate) (PEG-*b*-PDMAEMA) block copolymers synthesized by atom transfer radical polymerization (ATRP). The application of DNQ as a NIR-triggerable moiety was demonstrated by the release of the hydrophobic fluorescent dye, Coumarin 102, wherein the highest release efficiency was observed at acidic pH (protonation of the hydrophobic PDMAEMA core) [68]. In order to develop a localized drug delivery system with rationally controlled drug release and intelligent functionality, Kim and co-workers developed a tailorable, fibrous, site-specific drug delivery platform based on the NIR- and pH- responsive polymer poly(pyrrole) (PPy). The poly(pyrrole), when functionalized onto a Paclitaxel (PTX) loaded polycaprolactone (PCL) mat, enhanced the permeability of the fiber through NIR-induced heating, leading to accelerated release of PTX. Retarded but sustained release was observed after cessation of light exposure. The potential for spatially controlling drug release was evidenced by significantly lower rates of release observed in fibers not exposed to light. *In vivo* photothermal tests were carried out using PPy-coated membranes in a xenograft mouse model. Mats were locally implanted into mouse breast cancer (MCF-7)-bearing mice and subsequently subjected to 808 nm laser irradiation. Treatment with PCL-PTX/PPy under NIR irradiation quickly reduced the tumor sizes compared with the initial treatment due to the rapidly induced hyperthermia together with the NIR-activated PTX release, demonstrating that the NIR-responsive nature of PPy plays an important role in the tumor reduction [69].

The NIR-induced heating effect was also utilized by Agarwal, Jin and co-workers who incorporated IR780 as a photothermal agent into polymeric micelles composed of poly(ethylene glycol)-*b*-poly(*N*-acryloylglycinamide-*co*-acrylonitrile) (PEG-*b*-P(NAGA-*co*-AN)). The amphiphilic block copolymer exhibited an upper critical solution temperature; NIR-induced heating led to solubilization of the NAGA-*co*-AN block resulting in the complete release of the loaded doxorubicin. The *in vivo* property of the synthesized nanocarriers was tested in nude mice bearing MCF-7/DOX tumors as the xenograft model. Results displayed that the synthesized nanocarriers could efficiently inhibit MCF-7/DOX tumor growth and no obvious side effect was observed in tumor-bearing nude mice [70]. In addition to conventional approaches of externally triggering drug release, the photothermal effect can also be utilized to effect gene expression as demonstrated by Wang and co-workers. In this example, the NIR-induced photothermal effect was provided by a conjugated polymer nanoparticle, which was further modified with a positively charged peptide (Tat). The peptide confers the nanoparticles the capacity to coat the surface of living cells; subsequent NIR irradiation leads to localized heating leading to hyperthermic cytotoxicity as demonstrated on

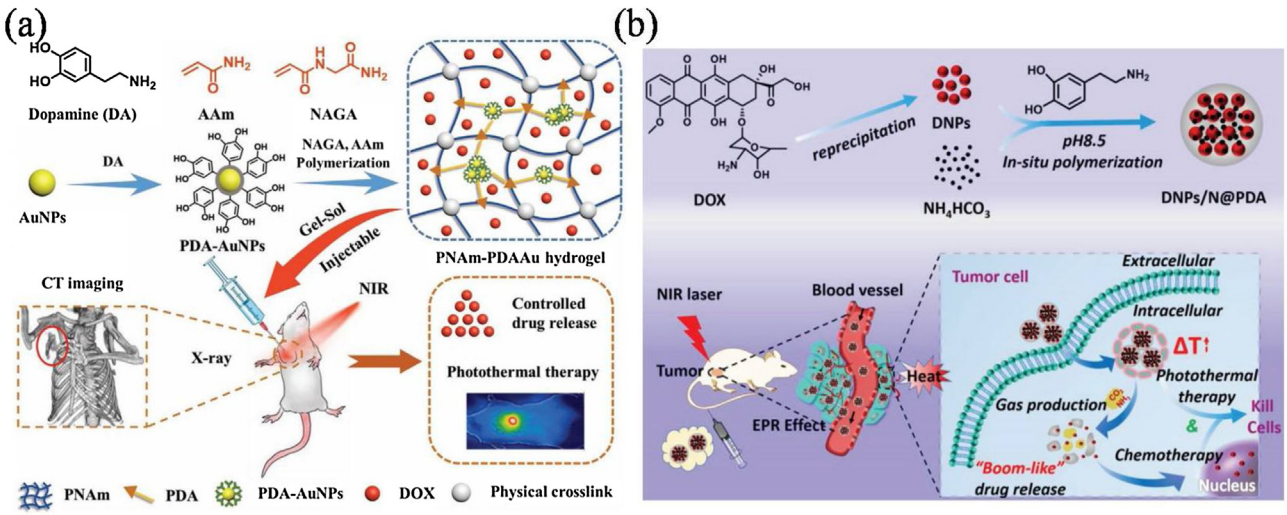

Fig. 1. (a) Schematic illustration for the fabrication of nanocomposite PNAm-PDAAu polymer hydrogel and the remotely controlled drug release of doxorubicin under NIR light [71], Copyright 2018. Reproduced with permission from WILEY-VCH Verlag GmbH & Co. KGaA, Weinheim. (b) Fabrication of polydopamine-coated and NIR-responsive carrier-free "nanobomb" (DNPs/N@PDA) based on packing the DNPs and NH_4HCO_3 with polydopamine (PDA) and schematic illustration of the stable blood circulation of DNPs/N@PDA and on demand "bomb-like" drug release. [72], Copyright 2018. Reproduced with permission from WILEY-VCH Verlag GmbH & Co. KGaA, Weinheim.

HeLa cells. Furthermore, the photothermal effect was also demonstrated on heat shock proteins, which was used as a promoter to drive the expression of EFGP (enhanced green fluorescent protein) [66]. Keurentjes and co-workers indicated that the large variation in diffusivity occurring near the glass transition temperature T_g of a polymer can be utilized to adjust drug release by thermal triggering mediated by a quaterrylenebis(dicarboximide) dye [65]. Thus, they placed compounded strands of polymer oversaturated with ibuprofen in a water bath to investigate the effect of temperature on the release of ibuprofen near the T_g of poly(*D, L*-lactic acid) (PLDL; T_g midpoint =56 °C, T_g trajectory = 50–60 °C). Poly(butyl methacrylate-*stat*-methyl methacrylate) (PBMA-MMA) was applied as the polymer matrix which contained 40 wt% ibuprofen. To remotely induce the required temperature change, NIR was applied as the external trigger. The off-situation was characterized by a low release rate (< 0.01 μg min^{-1}), whereas the high release rates of approximately 8–10 μg min^{-1} were obtained in the on-state, leading to on/off ratios of more than 1000. Release of ibuprofen below T_g was extremely low, which could be attributed to the spontaneous formation of a glassy surface layer, whereas in the rubbery state (> T_g) ibuprofen readily diffused out of the implant. The NIR-induced photothermal effect provided by gold nanoparticles was utilized by Liu and co-workers who embedded poly(dopamine) coated gold nanoparticles (PDA-AuNPs) within a poly(*N*-acryloyl glycinamide-*co*-acrylamide) PNAm-PAAm copolymer hydrogel (Fig. 1a). NIR-laser irradiation durations as low as 5 min was able to induce an increase in temperature to 68 °C and resulted in a gel-sol transition, which was exploited for the release of the model anticancer drug, doxorubicin. Perhaps more interestingly, excellent photothermal performance was retained *in vivo* even after 72 h of implantation, which was attributed to the strong binding of the polydopamine-coating to the hydrogel matrix [71]. In order to maximize drug loading efficiency and minimize the side effects introduced by the delivery system, Liu, Jia and co-workers synthesized doxorubicin nanoparticles that were coated with a thin film of polydopamine in the presence ammonium bicarbonate (DNPs/N@PDA) (Fig. 1b). The author's strategy was to utilize the NIR-laser induced photothermal heating of the polydopamine film to decompose the co-loaded NH_4HCO_3 into CO_2 and NH_3 gases and the generated gases would facilitate the breakdown of the thin polydopamine film leading to the 'bomb-like' release of the doxorubicin. Moreover, the NIR-responsive 'bomb-like' carrier-free DNPs/N@PDA nanoparticles demonstrated superior *in vitro* and *in vivo* therapeutic efficacy against the selected mice bearing Hela tumor [72].

The photocleavage of *o*-nitrobenzyl moieties is an often-utilized route to implement light-triggerable drug release. However, their absorption in the UV and visible wavelengths hinders tissue penetration and can potentially damage the skin. To utilize the more biologically favorable and penetrative wavelengths in the NIR region, Gu and co-workers loaded the hydrophobic NIR-absorbing dye, cypate (Ex/Em: 780/808 nm), into the core of chitosan-based micelles containing *o*-nitrobenzyl moieties in the hydrophobic block (Fig. 2a). Under NIR irradiation (765 nm), the cypate dye molecules emit 808 nm light, which can lead to the uncaging of the *o*-nitrobenzyl moieties *via* a two-photon process. The localized light emission of the two-photon wavelength (808 nm) enabled accelerated photocleavage of the *o*-nitrobenzyl moieties in comparison to direct irradiation with a 808 nm light source [73]. The cytotoxicity of the *o*-nitrobenzyl conjugated chitosan micelles was also investigated. The results demonstrated that the chitosan-based micelles containing *o*-nitrobenzyl moieties did not cause appreciable abnormalities in the subjected mice and even the group with the highest dosage (100 mg kg^{-1}) exhibited a death rate of zero. Additionally, none of the *in vivo* experimental mice exhibited unusual responses compared with the controls. The toxicity investigation suggested that the toxic effect of the synthesized micelles was not observed in the normal dose group of mice. Therefore, further experiments were carried out to confirm the toxicity of micelles on the organs of the subject animals, including liver, kidney, spleen, heart and lung. All toxic studies indicated that the chitosan-based micelles containing *o*-nitrobenzyl moieties exhibited none or low toxicity at the normal dosage without the NIR irradiation. However, upon NIR irradiation of the pathological tissues, photocleavage of the micelles resulted in damage induced by the nitrosaldehyde to the surrounding tissues and thereby enhanced the therapeutic efficacy of the drug delivery system [73]. Fluorescent carbon nanoparticles (FCNPs) are semiconductor quantum dots gaining increasing attention due to their bright photoluminescence and NIR-inducible photothermal activity. Zhou and co-workers explored the latter property for implementing NIR-triggerable drug release. The FCNPs were embedded into nanogels formed by a one-pot free radical precipitation copolymerization of *N*-isopropylacrylamide and acrylamide. The thermoresponsiveness

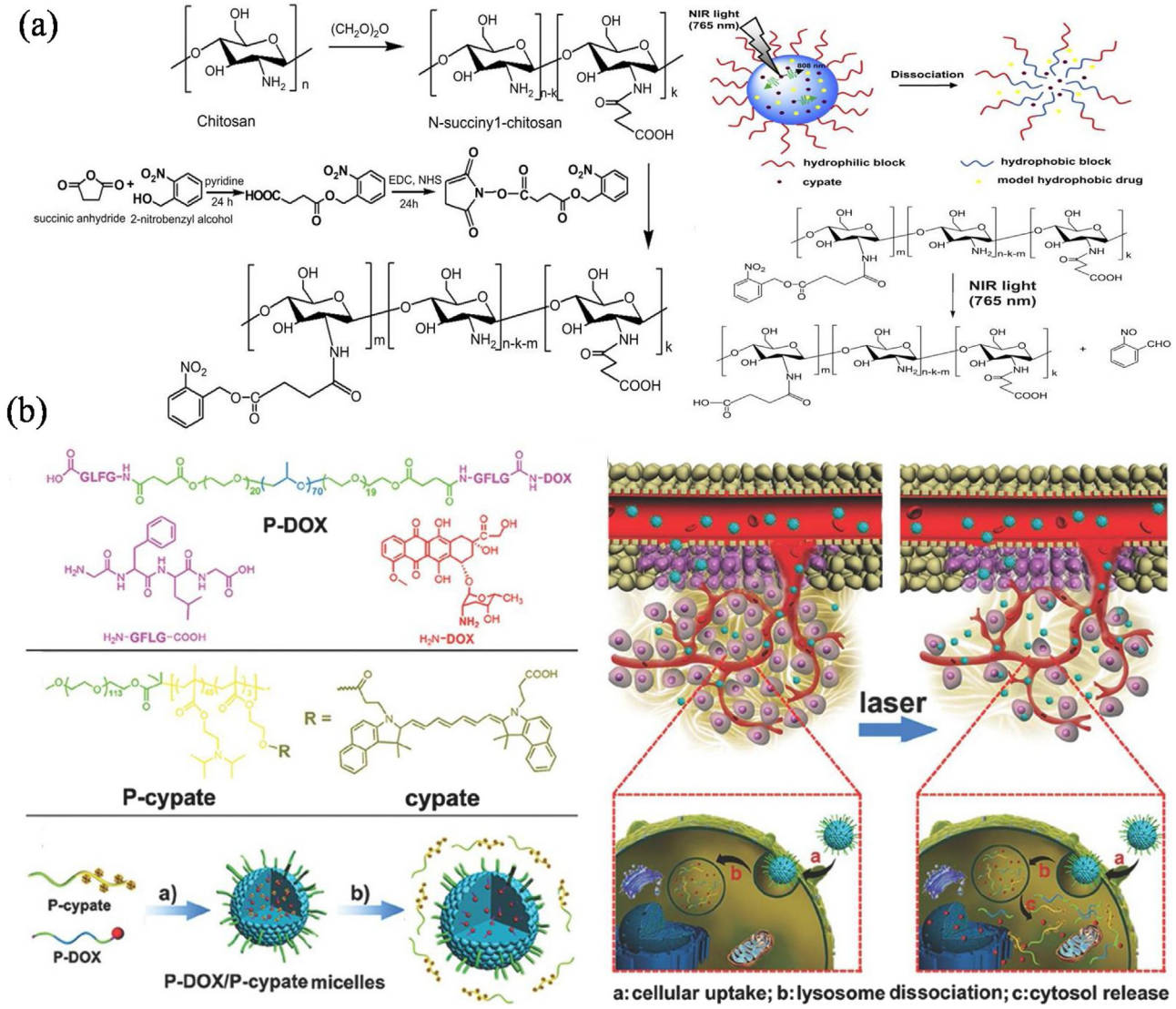

Fig. 2. (a) Schematic illustration of using NIR light excitation of Cypate to trigger dissociation of *N*-succinyl-*N*′-4-(2-nitrobenzyloxy)-succinyl-chitosan micelles. [73], Copyright 2013. Reproduced with permission from Elsevier Science Ltd. (b) Left: chemical structures of DOX prodrug, P-cypate diblock copolymer and P-DOX/P-cypate micelles. a) P-DOX and P-cypate diblock copolymer formed self-assemble micelles; b) the micelles dissociated at acidic condition due to protonation of PDPA tertiary amino groups. Right: scheme illustration for the controlled drug release induced by NIR laser irradiation. [77], Copyright 2015. Reproduced with permission from WILEY-VCH Verlag GmbH & Co. KGaA, Weinheim.

of the nanogel could be modulated by the localized photothermal effect provided by the FCNPs under NIR irradiation, which led to accelerated release of the model drug, curcumin [74].

Microcapsules embedded with gold nanorods were synthesized by He et al. *via* a layer-by-layer assembly of chitosan and alginate polysaccharides. The structure of lipid membrane and polyelectrolyte multilayers can be deconstructed by the increased temperature induced by NIR light. Interestingly, the photothermal effect of the gold nanorods upon NIR-laser irradiation was theoretically simulated to be localized to the nanometer range and therefore unable to cause hyperthermia towards cells. Thus, low energy (0.6 J cm^{-2}, 5 min) NIR-laser light triggered deconstruction of the microcapsules and enabled fast release of doxorubicin only. *In vivo* antitumor studies demonstrated that the synthesized microcapsule effectively prevents tumor growth and metastasis [75]. In another work by Lim's group, an efficient method was reported to prepare core-crosslinked micelles with NIR-triggerable drug release. The NIR-trigger system was based around the production of reactive oxygen species (ROS) by the NIR-absorbing dye, indocyanine green. Under NIR irradiation, the produced ROS would oxidize the diselenide crosslinks within the hydrophobic core, resulting in release of encapsulated doxorubicin [76]. In another work, Yu and co-workers incorporated the dye, cypate, as the NIR-responsive component in their micellar drug delivery system (Fig. 2b). A mild hyperthermic effect ($\Delta T = 5–10\,^{\circ}C$) was carefully tuned by selecting a cypate concentration of 150 $\mu g\,mL^{-1}$ and a laser intensity of 24 W cm^{-2}, to avoid heat degradation of cytoskeletal proteins. In this manner, NIR laser illumination enabled doxorubicin release in the cytoplasm; increased tumor penetration was attributed to mild hyperthermia and was followed by micelle dissociation and subsequent drug release in the acidic tumor microenvironment. The result of this approach was a greater than 50% reduction in viability of incubated MCF-7/ADR cells. By contrast, micelles with no loaded doxorubicin exhibited no decrease in the cell survival rate; phototoxicity was therefore attributed to the hyperthermia-triggered drug release [77].

2.1.2. *Visible light responsive systems*

Although more susceptible to scattering in biological tissues than NIR light, wavelengths in the visible range are an attrac-

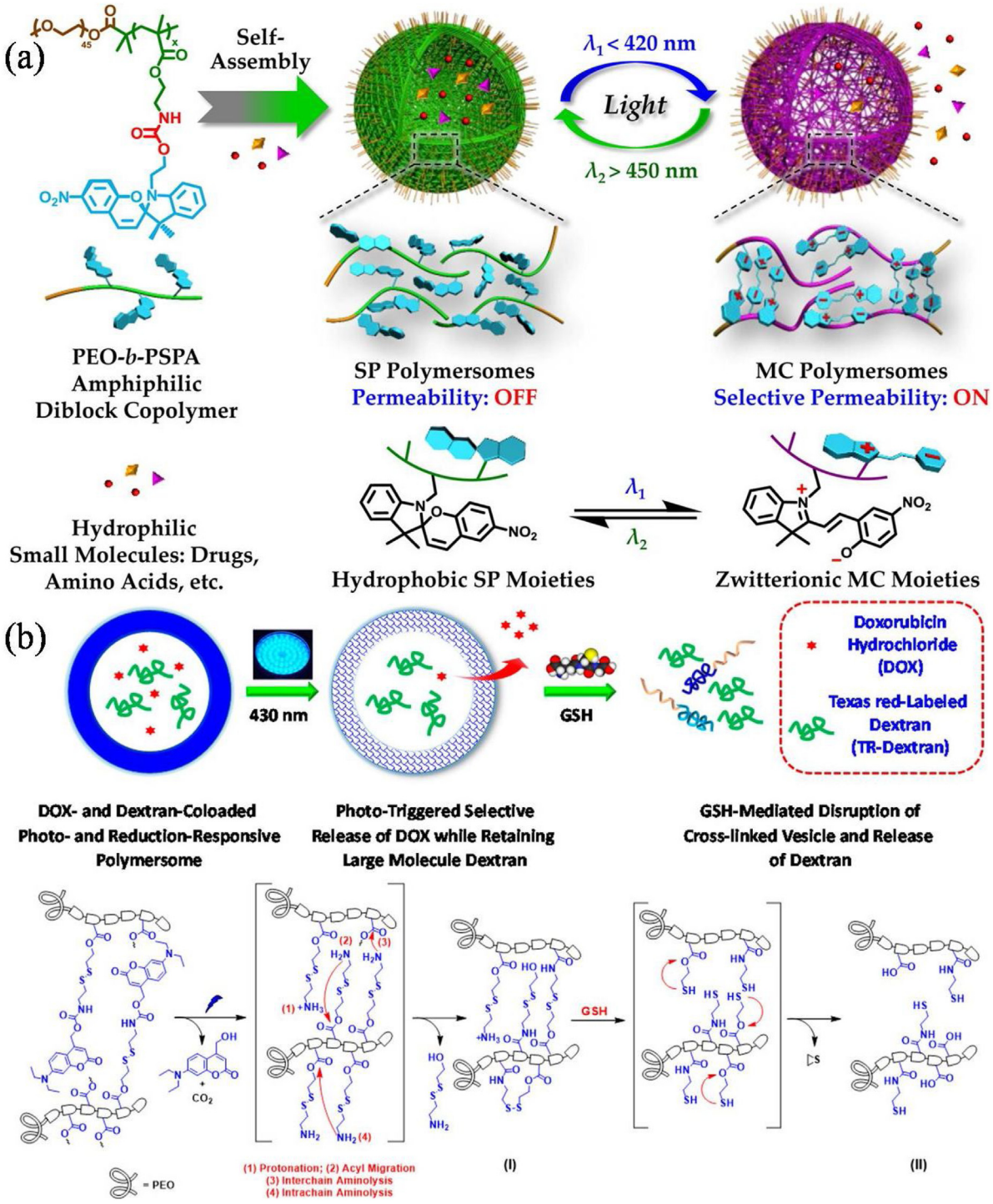

Fig. 3. (a) Amphiphilic PEO-*b*-PSPA diblock copolymers self-assemble into polymersomes with hydrophobic bilayers containing carbamate-based hydrogen bonding motifs. Spiropyran moieties within polymersome bilayers undergo reversible photo-triggered isomerization between hydrophobic spiropyran (SP, λ_2 > 450 nm irradiation) and zwitterionic merocyanine (MC, λ_1 < 420 nm irradiation) states. [78], Copyright 2015. Reproduced with permission from the American Chemical Society. (b) Schematic illustration for the fabrication of photo-responsive polymersomes for the sequential release of small and large molecule payloads. Upon irradiation with visible light, the photo-sensitive coumarin moieties are cleaved with the generation of highly reactive primary amine groups, which primarily undergo (1) protonation, (2) intramolecular acyl migration and (3–4) intra/interchain amidation reactions and the interchain amidation reactions thus crosslink the bilayer membranes (I). The traceless cross-linking process with a drastically enhanced permeability within the bilayer membranes leads to the selective release of small molecule payloads. A further addition of glutathione results in the disruption of the polymersomes due to the scission of reduction-responsive disulfide linkages (II) and subsequent release of large molecule encapsulants. [79], Copyright 2018. Reproduced with permission from the American Chemical Society.

tive trigger for drug release; one-photon visible light processes are more efficient than two-photon NIR excitations and at the same time less harmful to biology when compared to UV irradiation. Chromophores that undergo reversible isomerizations make for attractive triggers due to the potential switchability of the process. In the work of Liu and co-workers, photoisomerizable spiropyran moieties were introduced into self-assembled poly(ethylene oxide)-*b*-PSPA (PEO-*b*-PSPA) block copolymers *via*

polymerization of a spiropyran-based methacrylate (Fig. 3a). The initially hydrophobic spiropyran was photoswitched into a zwitterionic merocyanine under UV-irradiation (λ = 365 nm); this photo-induced hydrophobic to zwitterionic switch resulted in permeability of the polymersome bilayer. Conversely, the visible light irradiation (λ = 530 nm) reverted the merocyanines back to their hydrophobic spiropyran forms and in doing so reversed the bilayer permeability. The value of polymersomes with reversibly photo-switchable permeability was demonstrated by the spatiotemporally controlled release of a cell nuclei DNA-intercalating dye (DAPI, 4′,6-diamidino-2-phenylindole) in the presence of living HeLa cells [78]. In another work by Liu and co-workers, sequential drug release was demonstrated by combining a visible light responsive photocage with redox mediated decrosslinking (Fig. 3b). The authors synthesized dual stimuli-responsive amphiphiles consisting of the disulfide linkages (reduction responsive) and coumarin moieties (photosensitive) in the hydrophobic segment. The amphiphiles were self-assembled in the presence of doxorubicin to form large compound micelles and vesicles. Upon irradiation with visible light, primary amines were generated *via* the uncaging of the coumarins, leading to the aminolysis of the backbone esters (hydrophobic) to amides (hydrophilic). This change enabled the selective release of the encapsulated small molecule (doxorubicin) whilst retaining the larger molecule (dextran). Subsequent incubation with glutathione, a reducing agent that is found in abundance within the cytosol of cancer cells, reduced the disulfide crosslinks and ultimately led to the "traceless" disassembly of the drug delivery vehicles [79].

In a recent work, Wang's group reported the use of donor-acceptor Stenhouse adducts (DASA) to mediate the visible light triggered release of doxorubicin, camptothecin or Cy5 (dye) separately (Fig. 4) [80]. Under visible light irradiation (λ = 550 nm), DASA undergoes ring-closing from a colored, hydrophobic, conjugated triene to a colorless, cyclic, zwitterionic structure. When incorporated into nanoprecipitated nanoparticles, the phototriggered hydrophobic to hydrophilic transition resulted in swelling of the nanoparticles (influx of water molecules) under irradiation and consequently opened up the nanostructure to facilitate release of the encapsulated drug molecules. In another work, Liu's group reported the design and preparation of self-immolative polymersomes that were self-assembled from poly(*N*,*N*-dimethylacrylamide)-*b*-poly(benzyl carbamate) block copolymers. The self-immolative polymer (undergoing cascade depolymerization) was photocaged with perylene-3-yl, 2-nitrobenzyl or disulfide moieties which responded to visible light (λ = 420 nm), UV light (λ = 365 nm), or a reducing environment respectively. Following a 30 min exposure to visible light, the benzyl carbamate block was observed by GPC and TEM to undergo depolymerization over a 6 h period [81].

In the work of Almutairi and co-workers, a photodegradable implant was prepared by the incorporation of a visible light photocage into the polymer backbone (Fig. 5a). The photocage, 2-(4′-*N*-dimethylamino-4-nitro-[1,1′-biphenyl]-3-yl(butane-1,4-diyl dicarbonyl (ANBB), undergoes rearrangement into an *aci*-nitro intermediate when irradiated in an aqueous environment. The dimethylamino moiety aids in deprotonation of this intermediate, which results in photocleavage by way of β-elimination to form a nitro-alkene, resulting in the degradation of the polymer to which it was attached. The viability of this phototrigger *in vivo* was demonstrated *via* the release of dexamethasone from a subcutaneous implant upon irradiating with blue light (λ = 400–500 nm) [82]. Forsythe and co-workers constructed PEG-based hydrogels with photodegradable nitrobenzyl moieties embedded into the network (Fig. 5b). However, instead of using conventional *o*-nitrobenzyl moieties, which require UV irradiation, the authors conjugated the photocage to chromophores such as perylene and 7-(diethylamino)coumarin; these chromophores extended the wavelength of activation to visible wavelengths. Combining gels containing visible light activated photocages with conventional nitrobenzyl photocages enabled wavelength selective (UV or visible) release of cells [83]. Kim and co-workers reported a visible light triggered delivery system mediated by a co-encapsulated photosensitizer, chlorine e6 (Ce6) (Fig. 5c). Such photosensitizers are utilized for photodynamic therapy (PDT) and exert their therapeutic effects *via* the formation of reactive oxygen species (ROS) such as singlet oxygen ($^1O_2$). In this work, the authors synthesized an amphiphilic diblock copolymer, PEG-*b*-PCL that contained a vinyldithioether linker in between. Singlet oxygen can directly react with the double bond of vinyldithioether to form an unstable dioxetane intermediate which undergoes spontaneous cleave. Thus, under visible light irradiation (λ = 660 nm), micelles containing both the photosensitizer, Ce6 and the anti-cancer drug doxorubicin, underwent disassembly *via* this mechanism and exerted cytotoxic effects to PC3 and HeLa cell lines [84]. A similar approach was adopted by Huang and co-workers who coated magnetite (Fe_3O_4) nanoclusters with a polymer blend consisting of chitosan, poly(vinyl alcohol) and low molecular weight polyethyleneimine by way of an oil-in-water emulsion. The photosensitizer, Rose Bengal, was electrostatically adsorbed onto the multiple amines (primary, secondary and tertiary) that were present on polyethyleneimine. Under red light irradiation (λ = 632 nm), ROS-mediated oxidation of the polyethyleneimine, weakens the electrostatic attraction and results in the release of the photosensitizer. The nanoparticles adsorbed photosensitizers were taken up by cells and demonstrated superior photodynamic therapy compared to free Rose Bengal; the short lifespan and limited diffusion of reactive oxygen species may be overcome by localized delivery. *In vivo* xenograft studies revealed that the nanoengineered light-switchable carrier could greatly augment its photodynamic therapy efficacy against multidrug resistant MCF-7/MDR (multidrug resistant MCF-7 subline) tumor as compared to free drugs, attributable to its efficient cellular uptake and intracellular trafficking [85].

2.1.3. Ultraviolet light responsive systems

Ultraviolet light has a long history of use as the high energy wavelengths enable a variety of bond breaking and isomerizations which facilitate meaningful transformations in various fields. Although the toxicity and poor tissue penetration of ultraviolet light makes it unsuitable for the vast majority of biomedical applications, its accessibility and the wide range of activatable moieties enables it to remain highly relevant for testing proof of concepts [86].

Liu and co-workers reported the preparation of block copolymer vesicles capable of increasing permeability upon irradiation without undergoing dissociation (Fig. 6a). The authors synthesized amphiphilic poly(ethylene oxide)-*b*-poly(2-nitrobenzyloxycarbonylaminoethyl methacrylate) (PEO-*b*-PNBOC) block copolymers, wherein the second block contained a 2-nitrobenzyl photocage. Upon irradiation, the initially hydrophobic monomer undergoes cleavage, releasing 2-nitrobenzaldehyde and carbon dioxide, transforming the monomer into the hydrophilic 2-aminoethyl methacrylate. Interestingly, at pH 7.4, the UV-triggered transformation does not result in vesicle disassembly; the authors attributed this to amidation reactions which crosslinks the vesicles, enabling the vesicles to retain their structure whilst at the same time increasing the hydrophilicity of the originally hydrophobic bilayer. As a demonstration of the drug delivery capabilities of this system, the authors loaded both hydrophilic and hydrophobic species; the hydrophilic drug, doxorubicin hydrochloride, was loaded into the vesicle interior whilst the hydrophobic dye Nile red was loaded into the hydrophobic bilayer. Ultraviolet irradiation led to immediate release of the

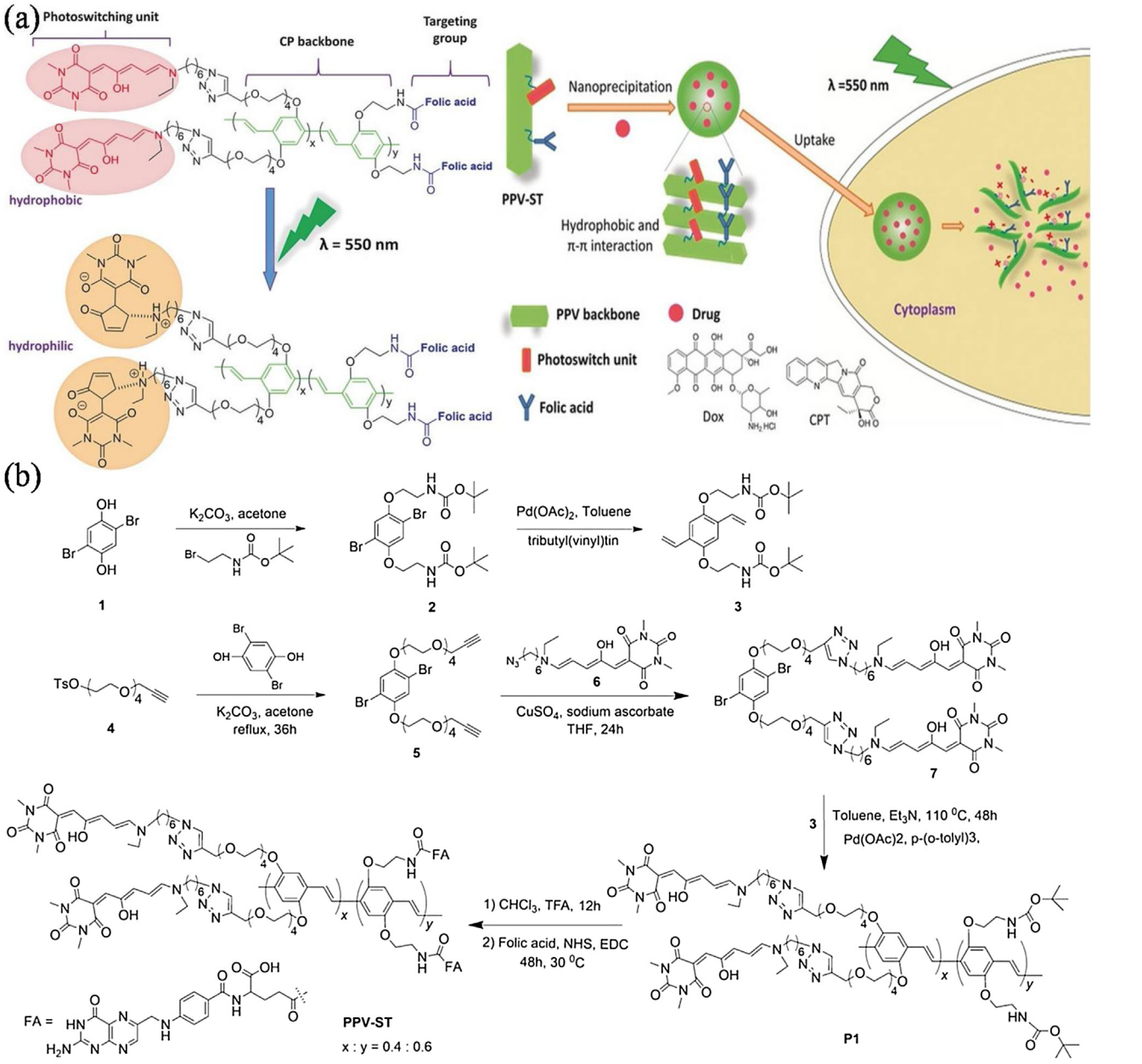

Fig. 4. (a) Schematic illustration for the fabrication of poly(*p*-phenylene vinylene) and the structural change leading to the drug release in cells under light irradiation (λ = 550 nm). (b) The synthetic route of conjugated polymer PPV-ST. [80], Copyright 2018. Reproduced with permission from WILEY-VCH Verlag GmbH & Co. KGaA, Weinheim.

hydrophobic Nile red (c.a. 80% in 30 min) while the hydrophilic doxorubicin hydrochloride was observed to be released at a much slower rate (hours) that was dependent on the duration of light exposure [87]. Li and co-workers reported dendrimer-core star polymers that contained spiropyran moieties in the peripheral segment to modulate the release of encapsulated species. Utilizing a polyester-based dendritic core, hydrophobic polycaprolactone arms were grown from the 16 hydroxyl functionalities. Thereafter, the terminal hydroxyls were esterified with an ATRP initiator for the polymerization of *tert*-butylmethacrylate; acidolysis to poly(methacrylic acid) and finally, partial esterification of spiropyran afforded the UV-responsive dendrimer star polymer which was self-assembled into micelles. Upon UV irradiation (λ = 365 nm), the colorless, closed-loop spiropyran, underwent ring-opening to a colored merocyanine, leading to purple micelle solutions. This photoresponsive trigger was further used to demonstrate cytotoxic doxorubicin release in the presence of 293 T cells [88].

Zhang and co-workers reported the preparation of star polymers where the fluorescence of the core-conjugated Camptothecin was quenched due to the nanomaterial surface energy transfer (NSET) effect originating from the co-loaded silver nanoparticles (Fig. 6b). As the Camptothecin was loaded *via* *o*-nitrobenzyl linkages, simultaneous drug release and fluorescence emission was achieved upon UV exposure (λ = 365 nm, 10 min) [89]. Yin and co-workers reported the self-assembly of three different helical poly(phenyl isocyanide)-*b*-poly(acrylate) block copolymers, wherein each block contained a caging moiety triggerable by UV light, oxidation or pH (Fig. 7). In this work, the UV-responsive moiety was again an *O*-nitrobenzyl moiety which could be uncaged into a primary amine; the increased hydrophilicity would cause micelle disassembly and concomitant release of species encapsulated in the hydrophobic core. Interestingly, exposing the micelles to all three stimuli (pH, UV and oxidation) simultaneously resulted in significantly faster release (15 h) of Nile

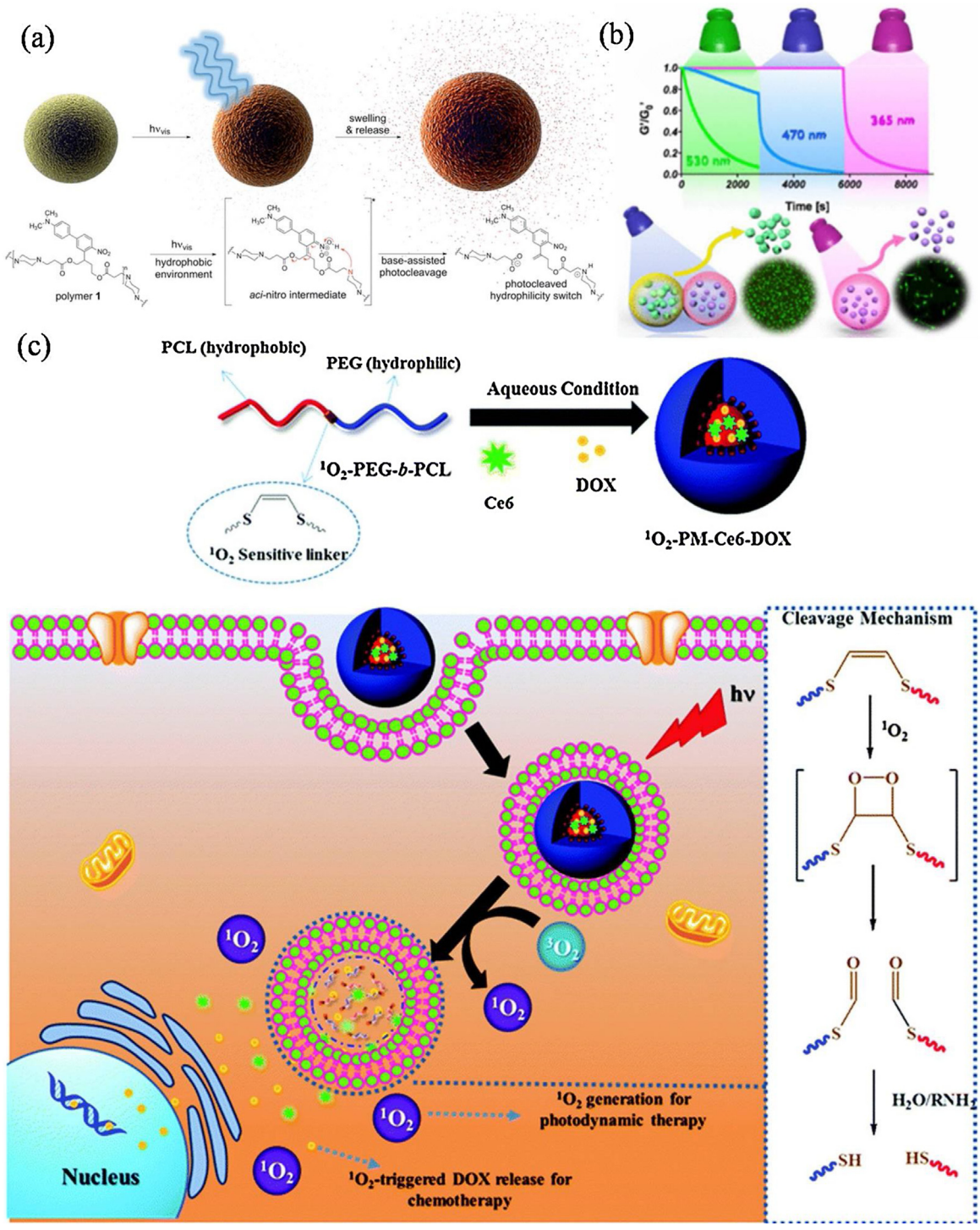

Fig. 5. (a) Visible light irradiation of particles composed of polymer 1 in aqueous media induces swelling and release of molecular cargo. Tertiary amines within the polymer backbone assist deprotonation of the *aci*-nitro intermediate in the hydrophobic particle microenvironment, leading to β-elimination and photocleavage in favor of photorearrangement. [82], Copyright 2015. Reproduced with permission from the Royal Society of Chemistry. (b) Schematic illustration for the fabrication of bio-orthogonal and photodegradable polymer hydrogels. [83], Copyright 2017. Reproduced with permission from the American Chemical Society. (c) Schematic illustration for the formation of Ce6 and DOX co-loaded polymer micelles, cellular uptake and visible light-triggered $^1O_2$-mediated intracellular co-delivery and on-demand release of Ce6 and DOX. [84], Copyright 2015. Reproduced with permission from the Royal Society of Chemistry.

Red compared to exposing the micelle to the three stimuli in sequence (> 35 h) [90].

Wang and co-workers employed spiropyran methacrylate as a phototriggerable moiety in the preparation of polymeric nanogels [91]. The hydrophobic spiropyran moiety could undergo photoisomerization to a hydrophilic merocyanine; the nanogels, which were composed of poly(acrylic acid-*co*-spiropyran methacrylate) crosslinked by *N*,*N*-bis(acryloyl)cystamine, became significantly more hydrophilic under UV irradiation. Doxorubicin, which was loaded into the nanogel by electrostatic interactions with the carboxyl moieties (acrylic acid), was observed to be released at rates dependent on the duration of UV irradiation (1–3 min). Further-

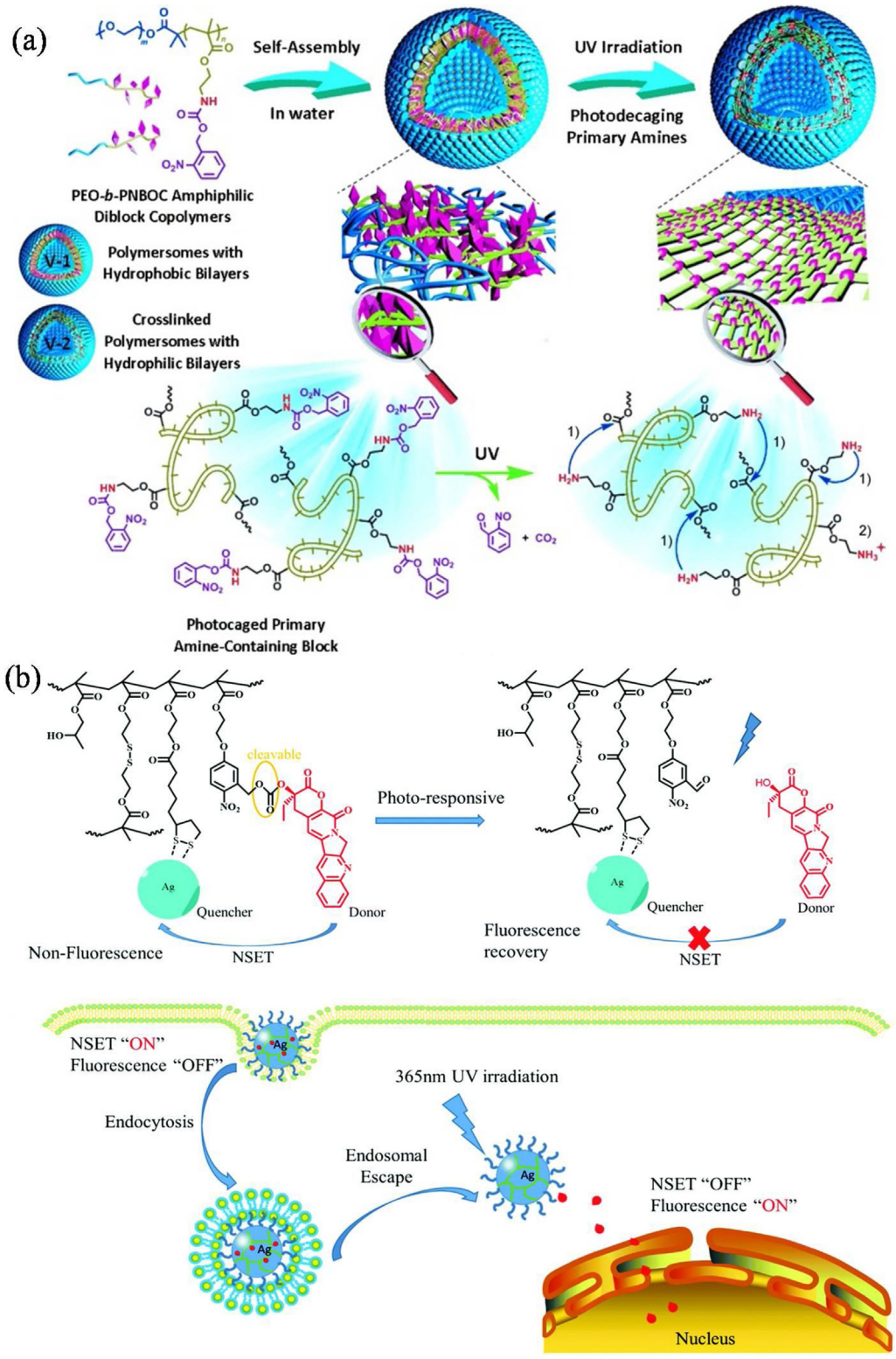

Fig. 6. (a) PEO-*b*-PNBOC amphiphilic BCPs self-assemble into polymersomes with the hydrophobic bilayer containing carbamate-caged primary amine moieties. UV irradiation triggers decaging reactions and the release of primary amine functionalities, prominent amidation reaction then occurs because of a suppressed amine pK_a within the hydrophobic vesicle membrane, resulting in vesicle crosslinking instead of vesicle-to-unimer disassembly. [87], Copyright 2014. Reproduced with permission from WILEY-VCH Verlag GmbH & Co. KGaA, Weinheim. (b) Illustration of the nanomaterial surface energy transfer effect of AgNPs coated by the CPT-based polymeric prodrug. The fluorescence of CPT tethered to the surface of AgNPs is quenched (fluorescence "OFF"), while the fluorescence recovers when CPT is released in response to UV irradiation (fluorescence "ON"). [89], Copyright 2018. Reproduced with permission from the Royal Society of Chemistry.

more, drug release could also be effected under reducing or acidic environments due to the disulfide crosslinking and electrostatic drug-nanogel interactions respectively. In a follow up, the same group copolymerized spiropyran methacrylate with the thermoresponsive *N*-isopropylacrylamide and subsequently self-assembled the chains into micelles [92]. As expected, the micelles were

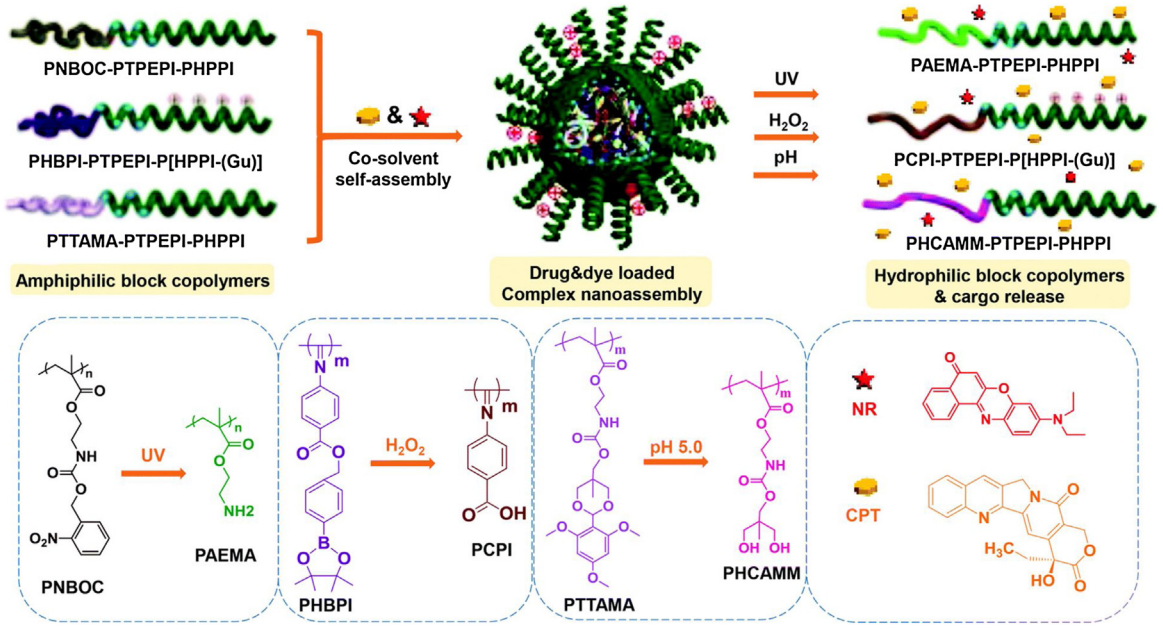

Fig. 7. Schematic illustration for the co-solvent self-assembly of light-responsive PNBOC-PTPEPI-PHPPI, pH-responsive PTTAMA-PTPEPI-PHPPI and H_2O_2-responsive PHBPI-PTPEPI-P[HPPI-(Gu)] copolymers as well as stimuli-triggered drug release. [90], Copyright2018. Reproduced with permission from the Royal Society of Chemistry.

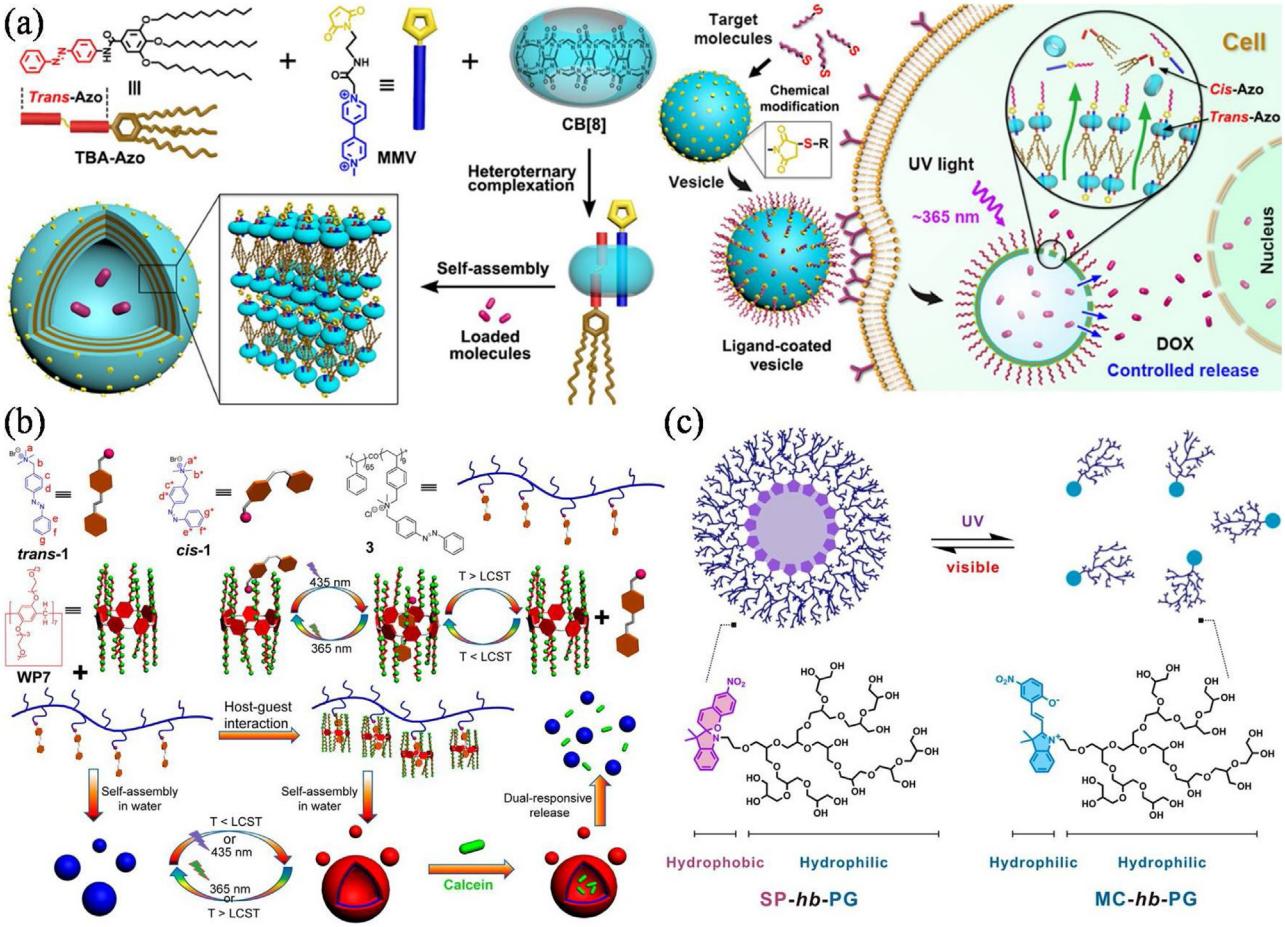

Fig. 8. (a) Left: schematic representation of the assembly strategy to construct supramolecular vesicles by supra-amphiphiles based on photoresponsive CB [8] heteroternary complexation. Right: schematic illustration of targeted and photocontrolled intracellular drug delivery through surface modification and UV light irradiation of supramolecular vesicles [93], Copyright2018. Reproduced with permission from the American Chemical Society. (b) Schematic illustration for the synthesis of supramolecular vesicles and the step-wise procedures of responsive controlled payloads release. [94], Copyright 2015. Reproduced with permission from the American Chemical Society. (c) Illustration for light-responsive micelle assembly and disassembly of spiropyran-hyperbranched-poly(glycerol). [99], Copyright 2014. Reproduced with permission from the American Chemical Society.

observed to release loaded coumarin 102 upon UV irradiation; as the spiropyran could also be protonated to form the hydrophilic merocyanine, accelerated release was observed under acidic conditions. Macromolecular supraamphiphiles represent a series of amphiphiles whose hydrophilic and hydrophobic segments bond through noncovalent interactions. Recently, giant supramolecular vesicles were prepared by hierarchical self-assembly of cucurbit [8] uril (CB [8])-based supraamphiphiles by Liu's group. Under UV irradiation, the supraamphiphiles were dissociated to achieve remote controlled drug release and resulted in significant apoptosis of tumor cells (Fig. 8a) [93]. A novel molecular recognition motif utilizing the water-soluble pillar [7]-arene and an azobenzene derivative as shown in Fig. 8b was reported in an earlier study by Huang and co-workers [94]. The reversible transformations of the synthesized vesicle morphologies could be regulated by the solution temperature or UV–vis light irradiation, enabling the remotely controlled release of the water-soluble calcein dye. This work provides a novel strategy to combine the polymer with pillararene supramolecular motifs for the construction of functional nanomaterials. Nitrobenzyl moieties were also explored by Sullivan and co-workers who incorporated this often-used functionality as a photo trigger for siRNA release. Cationic nitrobenzyl moieties contained in a mPEG-*b*-poly(5-(3-(amino)propoxy)-2-nitrobenzyl methacrylate) [mPEG-*b*-P(APNBMA)] were complexed with anionic siRNA and poly(acrylic acid) to form polyplexes, along with carboxyl-functionalized quantum dots as excipients. Under UV irradiation ($\lambda = 365$ nm) the nitrobenzyl moiety underwent photocleavage to form the corresponding carboxylic acid and nitrosobenzaldehyde; the generation of additional anions results in disruption of the complex and ultimately facilitated release of the siRNA. The enhanced stability of the polyplex, attributed to the anionic excipients, afforded an on/off like trigger which only facilitated gene silencing upon light exposure [95].

In contrast to the use of photocleavable moieties designed to release small molecules, Fan and Gillies reported self-assembled structures containing a hydrophobic poly(ethyl glyoxylate) segment which could undergo self-immolation *via* triggers such as a thiol reducing agent, UV light or H_2O_2 [96]. For the preparation of UV-induced self-immolative polymers, an *o*-nitrobenzyl moiety was placed at the junctions between the poly(ethyl glyoxylate) and the hydrophilic poly(ethylene oxide). Upon UV irradiation, the micelles formed from these block copolymers underwent cleavage to form separate hydrophilic and hydrophobic chains; the self-immolation of the hydrophobic poly(ethyl glyoxylate) resulted in an amplified release of hydrophobic species encapsulated such as Nile Red and Doxorubicin. Self-immolative polymers were also utilized by Almutairi and co-workers who copolymerized a monomer (based on the quinone-methide system) that was caged with 4,5-dimethoxy-2-nitrobenzyl alcohol, with adipoyl chloride [97,98]. Kim and co-workers reported micelles which could undergo UV-triggered disassembly using the hydrophobic to hydrophilic isomerization of spiropyrans (Fig. 8c) [99]. In this work, hyperbranched polyglycerols were grown from a single spiropyran species; as the hydrophobicity was solely based on the spiropyran, its isomerization to the hydrophilic merocyanine readily caused the disassociation of the micelles which could be reformed under 620 nm visible light. The drug delivery potential of this system was demonstrated by the release of hydrophobic pyrene species under 254 nm UV irradiation.

2.2. Microwave responsive systems

Microwave has been widely investigated and applied in biomedical fields as an external stimulus (with frequencies ranging from 300 MHz to 300 GHz) over the past decades [100]. Owing to its intrinsic heating capabilities, which can further elasticize, crosslink, coacervate or denature polymeric matrices, microwave attracts significant research interest and has been utilized to construct a variety of remotely controlled drug release systems [101]. Moreover, microwave-induced localized heating may also be used to selectively trap systemically introduced drug delivery vehicles by exploiting the lower critical solution temperature (LCST) transition [102]. However, it still remains a serious challenge to concentrate and focus microwave energy on tumorous tissue areas deep in body and to heat them selectively without adverse impact on surrounding healthy tissue. Moreover, one of the most limiting factors of microwave is the inherent attenuation of the electromagnetic waves spreading in tissues with high water content. Hence, there is an urgent need to develop nanocarriers exhibiting specific microwave responsivity to achieve efficient localized high intensity electric fields to avoid long time heating of the healthy tissues in body while generating enough heat in the nanocarriers to externally control drug release at the expected locations [104] (Table 2).

The use of microwaves to remotely trigger drug release is an attractive proposition as it is a noninvasive stimulus capable of deep penetration and heating with high thermal efficiency. However, compared to the use of light to extrinsically control drug release, delivery systems utilizing microwaves are still in an early stage of development. Yu and co-workers reported the first polymeric drug delivery system triggerable by microwaves, utilizing poly(*p*-phenylenendimine) (P*p*PD)/poly(*N*-isopropylacrylamide) (PNIPAM) core-shell microparticles for controlled drug release [102]. The P*p*PD core possessed the ability to convert absorbed microwaves to thermal energy; 50 s of heating under 2.4 GHz (120 W) microwaves caused the core shell nanoparticles to reach a temperature of 62 °C from an initial temperature of 25 °C. Critically, under 10 s of microwave induced heating, the core shell nanoparticles were observed to release the folic acid payload in a burst. The utilization of microwaves as a remote trigger was demonstrated by the burst release of the folic acid payload. Cui and co-workers reported the design and synthesis of multifunctional composite nanoparticles comprised of an inorganic Fe_3O_4@ZnO@mGd_2O_3:Eu core that was covalently coated with a poly[(*N*-isopropylacrylamide)-*co*-(methacrylic acid)] P(NIPAm-*co*-MAA) copolymer. Under microwave irradiation (2.45 GHz), heating of the ZnO layer induced shrinkage of the outer polymer shell, resulting in the release of entrapped etoposide (VP16) from the mesoporous Gd_2O_3:Eu shell. The drug release of entrapped etoposide could reach 81.7% within 10 h of microwave irradiation with *in vitro* studies showing both the feasibility and advantage of remote-controlled drug release using microwaves (Fig. 9a) [103]. The encapsulation of sodium chloride (NaCl) has also been investigated as a route to confer microwave responsivity. Dai and co-workers prepared vesicles composed dipalmitoyl-*sn*-glycero-3-phosphocholine (DPPC) cholesterol and 1,2-distearoyl-*sn*-glycero-3-phosphoethanolamine-*N*-methoxy(polyethylene glycol)-2000 (DSPE-PEG_{2000}) *via* the thin-film hydration method. Critically, the encapsulation of NaCl conferred a microwave-induced thermal effect; under 2 min of microwave irradiation (450 MHz, 1.8 W), temperatures were observed to increase by 12.5 °C. As a consequence of the thermal effect, the DPPC, which possesses a phase-transition temperature of 41.5 °C, increased in permeability, resulting in the release of encapsulated NaCl and doxorubicin (>67.6%). Moreover, growth inhibition of the tumor injected with the synthesized liposomes was evaluated to be 73.4% under microwave irradiation (Fig. 9b) [104].

2.3. Magnetic field responsive systems

Among various inorganic-nanomaterials which are responsive to external magnetic fields, iron oxide nanoparticles (IONPs), which

Table 2
Summary of microwave triggered drug release *in vivo*/*vitro*.

Ref. Year	Irradiation protocol	Microwave-responsive system	Microwave-responsive release mechanism	Therapeutic agents and dose
[102] 2017	f = 2.4 GHz P = 120/360 W 50/30/10 sec	PpPD/PNIPAM core-shell particles	Absorb microwave irradiation and convert electromagnetic radiation to thermal energy	Etoposide 0.3 mg/mL Folic acid 5 mg/mL
[104] 2016	f = 450 MHz P = 1.8 W 120 sec	DOX&NaCl@DPPC-Chol-DSPE-PEG2000 liposomes	Microwave absorption and hyperthermia induced to increase lipid bilayer permeability	Doxorubicin 111.4 μg/mL
[103] 2015	f = 2.45 GHz 420 min	Fe_3O_4@ZnO@mGd_2O_3:Eu@P(NIPAm-*co*-MAA) core-shell particles	Polymer shrinks due to the generated heat from microwave	Etoposide 0.3 mg/mL

Table 3
Summary of magnetic field triggered drug release *in vivo*/*vitro*.

Ref. Year	Irradiation protocol	Magnetic-responsive system	Magnetic-responsive release mechanism	Therapeutic agents and dose
[123] 2018	2200 G 64 hours	P(VA-*co*-HEA) contained Fe_3O_4@Agarose NPs	Alignment of the magnetic nanoparticles expands the network	Doxorubicin 12 μg/mL
[127] 2017	f = 470 kHz 2 hours Amplitude = 18 mT	P(MEO_2MA-*co*-OEGMA-*co*-MAA) nanogels@γ-Fe_2O_3	Magnetic hyperthermia induces swelling-deswelling behavior of nanogels	Doxorubicin 1 mg/mL
[114] 2014	H = 8 kA m^{-1} f = 230 kHz 20 min	Fe_3O_4/DOX/PPy-PEG-FA NPs	Magnetic hyperthermia softens the polymer phase	Doxorubicin 0.13 mg kg^{-1}
[115] 2014	P = 5 kW 1 hour f = 230 kHz	PNIPAM coated PEG- Fe_3O_4 NPs	Magnetic heat and magnetic-mechanical vibrations inside hydrogels	Doxorubicin 0.2 mg/mL
[116] 2014	100 V 0.8 A 30 min 50 Hz	P(NIPAM-AAm)-BFNP nanogels coated IONPs	Magnetic hyperthermia induces swelling and shrinking of the gel	Curcumin 1 mg/mL
[120] 2014	H = 89.9 kA m^{-1} f = 114 kHz 20 min	PLA-*b*-P(*N*-isopropylacrylamide-*co*-*N*,*N*-dimethylacrylamide)@$Mn_{0.6}Zn_{0.4}Fe_2O_4$	Magnetic hyperthermia breaks the structure that contained thermo-sensitive polymer	Camptothecin 200 μg/mL of CPT/MTRNs
[113] 2013	P = 3.5 kW f = 330 kHz 2 days	P(NIPAAm-*co*-AAm)-*b*-PCL@Fe_3O_4 NPs	Magnetic hyperthermia medicates drug release based on thermo-sensitive polymer	Doxorubicin 1 mg/mL
[111] 2012	H = 2.5 kA m^{-1} f = 44.2 kHz 15 sec	PVA-(PEO-PPO-PEO)@Fe_3O_4 NPs	Magnetic hyperthermia induces the structure shrinkage and collapse	Ethosuximide 9.33 mg kg^{-1}
[122] 2012	H = 2.5 kA m^{-1} f = 50∼100 kHz 20 min	PLGA/DiO@IONPs@DOX	Magnetic hyperthermia medicates the volume or local voids of the PLGA shell	Doxorubicin 1 mg/mL
[124] 2012	H = 4/8/16 kA m^{-1} f = 50 kHz 10 min	PVA@Fe_3O_4 NPs	Magnetic hyperthermia medicates the morphology structure	Paclitaxel Doxorubicin 1.2 mg/mL

have already been approved by the US Food and Drug Administration (FDA), have attracted significant interest for a variety of applications due to their biocompatibility, low toxicity and ease of synthesis [105]. Due to their high surface area to volume ratios and superparamagnetic properties, IONPs are widely utilized as both contrast agents for magnetic resonance imaging (MRI) and remote controlled drug release under a magnetic field. Unfortunately, IONPs are susceptible to self-agglomeration, arising from their high surface energies. Additionally, they have a tendency to adsorb to proteins, which significantly limit their applications. To overcome these drawbacks, IONPs are surface-functionalized with functional polymers; the significantly improved dispersibility of the IONPs corresponds to an increase in their circulation duration [106]. Additionally, the surface tethered polymers afford opportunities to encapsulate or load therapeutic agents (drugs or genes), targeting ligands and/or permeation enhancers. A significant advantage of these paramagnetic materials is that they can induce localized heating under an external alternating magnetic field (AMF). The use of an AMF has attracted tremendous research interest owing to its deep penetration into tissue that is at the same time, less harmful in comparison to the ionizing effect X-rays. The usage of an AMF to induced spatially localized hyperthermia from magnetic nano-mediators is a promising therapeutic modality that has also attracted significant scientific attention. This AMF-generated magneto-thermal effect can be further applied as a secondary stimulus to trigger drug release in a spatiotemporal manner [107]. The design of a magnetically responsive drug delivery nanoplatform typically combines with a magnetic mediator, which transforms the magnetic energy into heat (such as IONPs), in combination with a thermoresponsive polymeric carrier to induce drug release [108]. Numerous drug release systems have been developed using this magnetically responsive strategy [109,110] (Table 3).

For example, Pluronic F-127 (poly(ethylene oxide)-poly(propylene oxide)-poly(ethylene oxide), (PEO-PPO-PEO)) was combined with polyvinyl alcohol (PVA) to form a nanoshell containing superparamagnetic iron oxide (Fe_3O_4) nanoparticles and the anti-epilepsy drug, ethosuximide (ETX). Critically, the hydrogen-bonding between the PVA and the PEO segments provided the structural integrity required for the formation of the nanoparticles, overcoming the tendency of the triblock copolymer to redistribute below its LCST. Localized heating induced *via* the application of a magnetic field (H = 2.5 kA m^{-1}, f =44.2 kHz) resulted in the shrinkage of the triblock copolymer, which occurred in tandem with the thermal expansion of PVA. Under heating, the nanocarriers were observed to undergo shrinkage, with a higher composition of the triblock copolymer leading to a greater decrease in the diameter; drug release

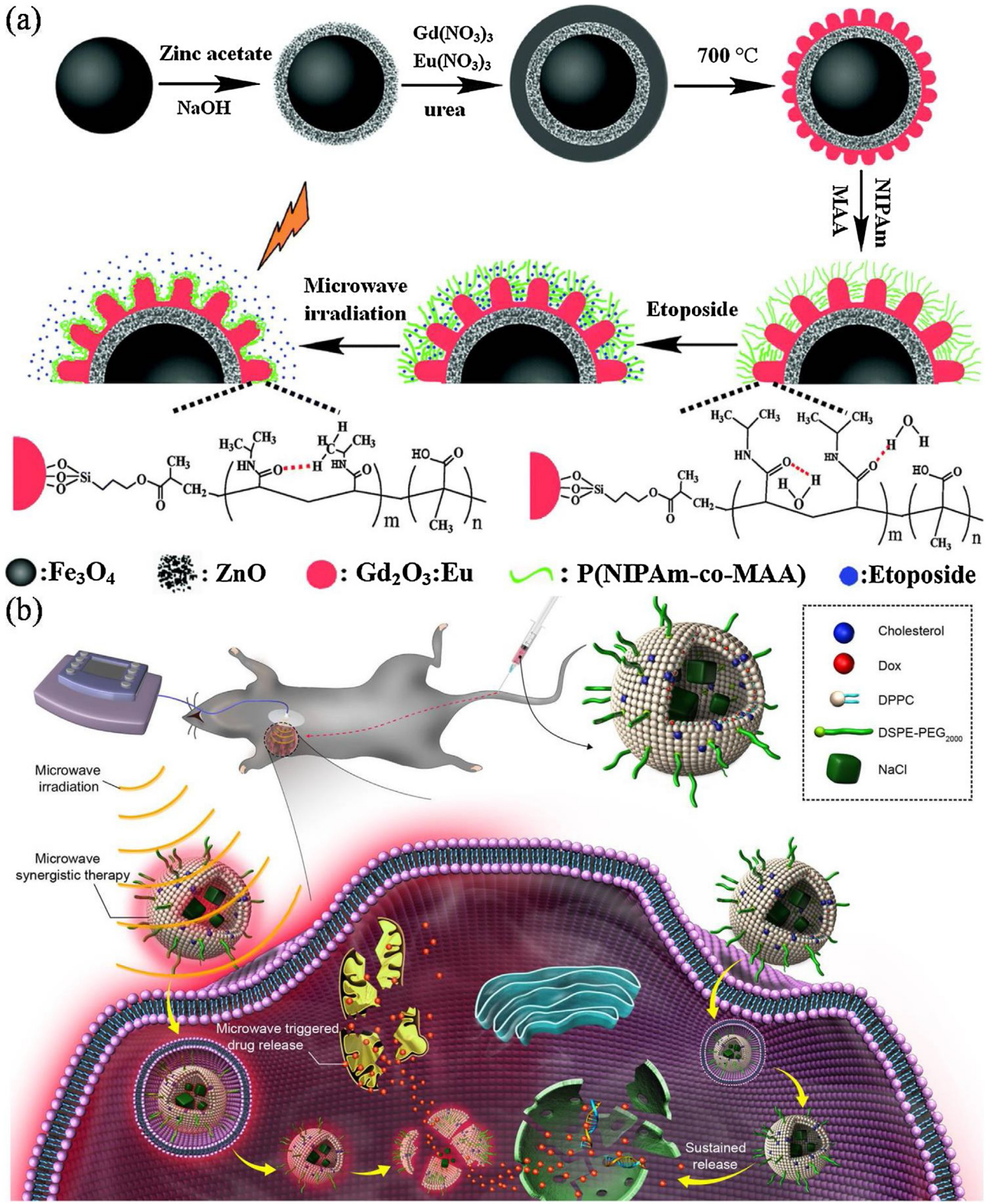

Fig. 9. (a) Schematic illustration showing the formation of multifunctional Fe_3O_4@ZnO@mGd_2O_3:Eu@P(NIPAm-*co*-MAA) nanocarriers and its controlled drug release under microwave. [103], Copyright 2015. Reproduced with permission from the Royal Society of Chemistry. (b) Schematic representation of the fabricated DOX&NaCl@liposomes applied as the nanocarrier for microwave triggered drug release. [104], Copyright 2016. Reproduced with permission from the American Chemical Society.

behavior followed this trend with burst release observed with higher shrinkage whilst sustained release occurred with lower degrees of shrinkage. Additionally, the *in vivo* study applying the Long-Evans rat model demonstrated that a significant reduction in the spike-wave discharge after the anti-epilepsy drug could be burst released from the synthesized thermosensitive nanocarriers [111].

Keurentjes and co-workers designed an implant responding to an externally applied alternating magnetic field for the triggered release of ibuprofen. Poly(methyl methacrylate) cylinders

(length =10 mm, diameter =3 mm) containing superparamagnetic iron oxide nanoparticles (EMG705; 30–50 wt%) were dip coated with a 0.3 mm matrix of poly(*n*-butyl methacrylate-*stat*-methyl methacrylate) (75 mol% *n*-butyl methacrylate; $T_g \approx 52\,^{\circ}C$) containing the ibuprofen (5–29 wt%). The alternating magnetic field strength of 2850 A m^{-1} (f=745 kHz) triggered up to 25-fold increase in Ibuprofen over the passive release rate, with the latter seemingly corresponding to the amount of plasticizing drug contained in the outer layer [112]. A system for multiple reversible on-demand drug release that can be activated by an alternating magnetic field as the external trigger was prepared by Keurentjes's group [109]. The synthesized core/shell material was developed based on a macroscopic spherical iron core coated with a thermoresponsive polymer poly(styrene-*stat*-butyl methacrylate) (p(S-BMA); $T_g \sim 45\,^{\circ}C$), containing ibuprofen as the drug. The release rate of ibuprofen was significantly increased (up to 35 times) when exposed to an alternating magnetic field. The iron core with the polymer coating was heated by the applied magnetic field. Moreover, the diffusion of ibuprofen was increased with the raised temperature, particularly around the glass transition temperature of the polymer. As expected, the drug release rate from the designed system was significantly increased during exposure to the magnetic field. Rozhkova and co-workers reported the encapsulation of superparamagnetic iron oxide nanoparticles measuring 11 nm in diameter inside micelles composed of poly(*N*-isopropylacrylamide-*co*-acrylamide)-*b*-poly(ε-caprolactone) (P(NIPAAm-*co*-AAm)-*b*-PCL) amphiphilic block copolymers. The random hydrophilic block possessed an LCST of 43 °C, while the hydrophobic PCL segment starts to soften from ~40 °C and eventually melts at 57 °C, providing stability at physiological temperatures (37 °C). The application of an external magnetic field, fixed at a frequency of 330 kHz, for 10 min. resulted in doxorubicin release that was 3 times higher compared to samples heated in a water bath to the same temperature, emphasizing the importance of the localized heating in facilitating drug release [113]. In an effort to maximize the heat conversion efficiency under an alternating magnetic field, Hayashi et al. reported a polymeric nanocarrier containing iron oxide nanoparticle clusters. The Fe_3O_4/DOX/PPy-PEG-FA nanoparticles possessed a glass transition temperature (T_g) of 44 °C. When a harmless alternating current magnetic field (H = 8 kA m^{-1}, f =230 kHz, Hf = 1.8 × 109 A m^{-1} s^{-1}) was applied, the polymer layer softened and resulted in the release of the doxorubicin cargo. The efficacy of these nanoparticles were demonstrated by *in vivo* studies wherein mice that were administered the nanoparticles and exposed to an alternating magnetic field for 20 min. were observed to be tumor free within 8 days with no recurrence for the remaining 45 days of the study [114].

Dravid and co-workers reported the preparation of poly(*N*-isopropylacrylamide) (PNIPAM) hydrogels for the encapsulation of PEG-functionalized iron oxide nanoparticles (d = 25 nm) as shown in Fig. 10a. Results demonstrated that the phase transition temperature of PNIPAM hydrogels was elevated to 40 °C due to the presence of encapsulated IONPs, which was more suitable for biomedical applications. Investigation of doxorubicin release behavior showed that application of a radio-frequency (RF) field (5 kW, f =230 kHz, 1 h) resulted in a two-fold enhancement over a 24 h period when compared to the control in which no RF was applied. *In vitro* studies using HeLa cell lines showed that the highest cytotoxicity arose from application of the RF field to the doxorubicin loaded hydrogels, signifying the need for remote triggering to effect therapeutic activity [115]. Zhou and co-workers prepared hybrid nanogels composed of a thermoresponsive poly(*N*-isopropylacrylamide-*co*-acrylamide) shell and contained a bifunctional nanoparticle wherein superparamagnetic iron oxide nanocrystals were clustered inside a porous carbon shell that was also decorated with fluorescent carbon dots. Aside from its NIR-responsivity *via* the carbon shell, drug release from the hybrid nanogel could also be triggered *via* the application of an alternating field; the resulting hyperthermic effect increased temperature, which could be utilized to trigger an enhancement over the passive release rate that subsided following cessation of the magnetic field [116]. Moreover, the combination of magnetic iron oxide nanoparticles and lipids for controlled drug release were also reported [117,118]. For example, Banerjee's group utilized thermosensitive magnetoliposomes comprised of 1,2-dipalmitoyl-*sn*-glycero-3-phosphocholine (DPPC) and 1-palmitoyl-2-oleoyl-*sn*-glycero-3-phospho-*rac*-glycerol (PG) (9:1, w/w) as drug carriers for the controlled release of paclitaxel. Application of an alternating magnetic field (10 kA m^{-1}, 423 kHz) raised the temperature from 25 °C to 43 °C, which was maintained for 30 min; over 55% of the encapsulated paclitaxel was released at 43 °C compared to only 1% at 37 °C, demonstrating an effective trigger for drug release [117].

Although the use of iron oxide nanoparticles to impart a magnetoresponsive trigger has featured prominently as evidenced by the majority of literature examples, including those presented above, nanoparticles with advantageous properties are slowly being investigated as alternatives. Landfester and co-workers reported the use of superparagmagnetic $MnFe_2O_4$ nanoparticles as the magnetoresponsive component in a nanocapsule prepared *via* an interfacial polyaddition in an inverse miniemulsion [119]. Interestingly, thermoresponsivity was provided by the azoinitiator, VA-060 (2,2′-azobis[2-[1-(2-hydroxyethyl)-2-imidazolin-2-yl]propane] dihydrochloride), which was polymerized into the shell *via* its hydroxyl moieties. In addition to its r_2 relaxivity, which makes it ideal as a negative MRI contrast agent, the $MnFe_2O_4$ nanoparticles provided heating when exposed to an alternating magnetic field (4.5 kA m^{-1}, 720 kHz); the water-soluble dye, sulforhodamine 101, which was loaded into the aqueous interior, was observed to release to a greater extent with increasing incorporation of VA-060. Li et al. reported the preparation of magnetoresponsive nanoparticles incorporating $Mn_{0.6}Zn_{0.4}Fe_2O_4$ nanoparticles which were combined with camptothecin into nanoclusters that were encapsulated inside amphiphilic polylactide-*b*-(*N*-isopropylacrylamide-*co*-*N*,*N*-dimethylacrylamide) (Fig. 10b). The hybrid nanoparticles provided high specific absorption rate (SAR) affording near complete release of the loaded campothecin within 10 min of being exposed to an alternating magnetic field ($H_{applied}$ = 89.9 kA m^{-1}, f =114 kHz) [120]. Schatz and co-workers investigated the use of lanthanum strontium manganese oxide (LSMO) nanoparticles as the magnetoresponsive trigger. The key feature of this work was that the Curie temperature (T_c) of the LSMO particles could be tuned; the $La_{0.82}Sr_{0.18}MnO_3$ nanoparticles utilized in this work possessed a Curie temperature of 42 °C, which prevents overheating (> 43 °C) which would otherwise damage healthy tissues. Due to the potential toxicity of the magnetic nanoparticles, the magnetoresponsive entities were coated with silica and subsequently coated with a combination of the double hydrophilic block copolymer, poly(ethylene oxide)-*b*-poly(L-lysine) and the thermoresponsive poly(ethylene oxide-*co*-propylene oxide)-*b*-poly(L-lysine). When exposed to an alternating magnetic field (108 kHz) for 2 h, release of the model drug, doxorubicin, was observed to be about five times higher than the passive release observed at 25 °C [121].

Sung and co-workers reported the development of magnetoresponsive hollow microspheres prepared by a double-emulsion approach (Fig. 11a) [122]. Iron oxide nanoparticles were embedded in the poly (D,L-lactic-*co*-glycolic acid) (PLGA) shell, which when exposed to an alternating magnetic field (2.5 kA m^{-1}, f = 50–100 kHz) would undergo heating above its T_g ($\approx$ 40 °C), causing the release of encapsulated doxorubicin. The distinguishing feature of this work was that the alternating magnetic field was turned off, allowing the PLGA shell to return to its glassy

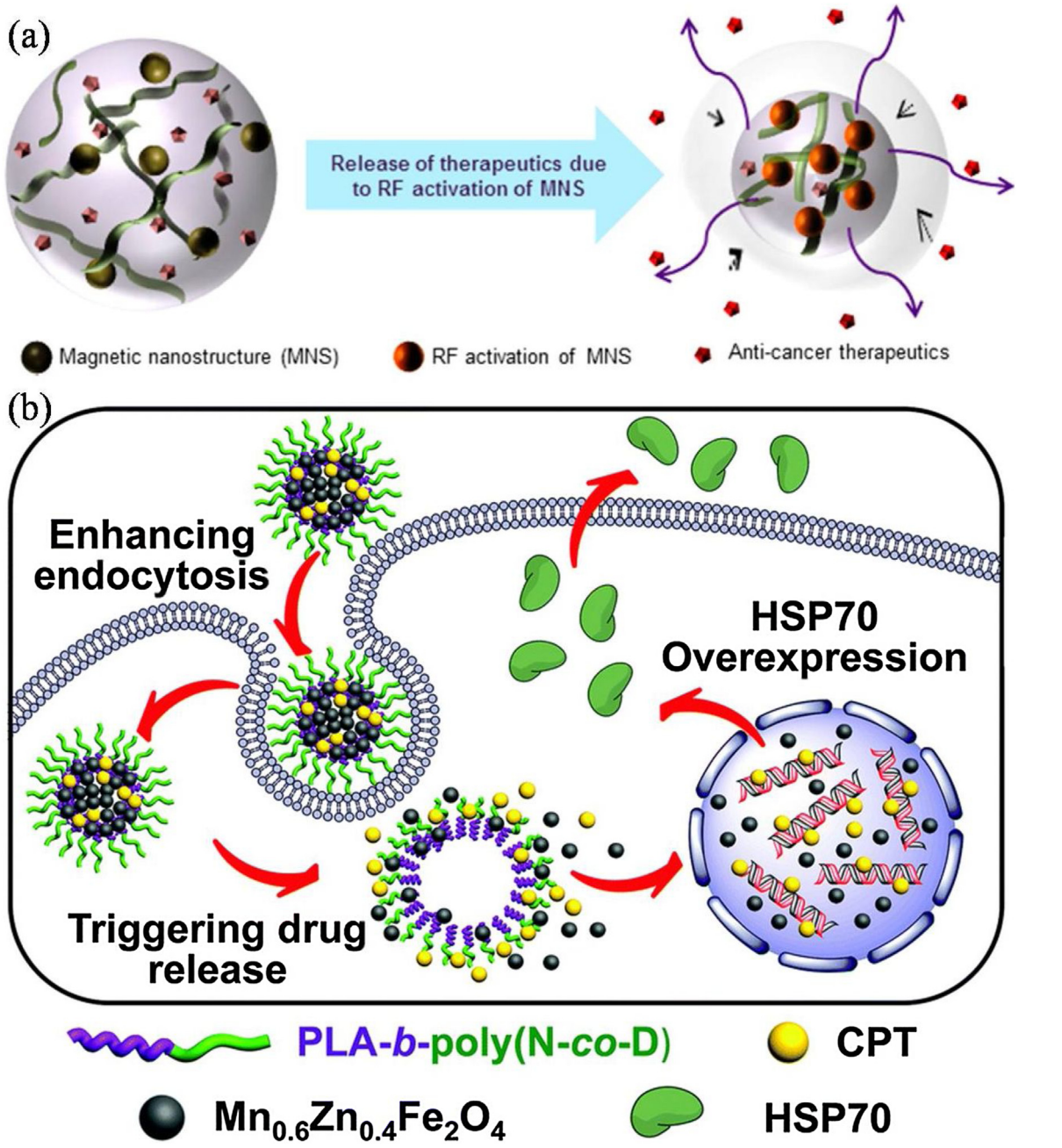

Fig. 10. (a) Schematic illustration showing thermo-responsive hydrogel's structural collapse with RF activation of MNS, thereby triggering the release of therapeutic cargo. [115], Copyright 2014. Reproduced with permission from the American Chemical Society. (b) Schematic illustration of synergistic mechanism between efficient magnetic hyperthermia and chemotherapy by magnetothermally-responsive nanocarriers, including enhancement of endocytosis and triggering drug release. [120], Copyright 2014. Reproduced with permission from the Royal Society of Chemistry.

state and thereby halt drug release; switching the alternating magnetic field between "ON" and "OFF" states afforded pulsatile release, enabling superior control over physiological drug concentrations. Dong and co-workers prepared hydrogels comprised of salecan-*g*-poly(vinylacetic acid-*co*-2-hydroxyethyl acrylate) [poly(VA-*co*-HEA)] and containing Fe_3O_4@Agarose nanoparticles. Fast release of doxorubicin was observed under acidic conditions (pH = 4.5); when combined with an external magnetic field, both an accelerated release rate and a higher total cumulative release was observed [123].

Magnetic core-shell water/oil/water nanocapsules were prepared by emulsification of iron oxide nanoparticles in the presence of poly(vinyl alcohol) (PVA) followed by solvent evaporation; hydrophilic doxorubicin was incorporated inside the core while hydrophobic iron oxide nanoparticles and paclitaxel were encapsulated within the shell [124]. To increase treatment efficacy, a peptide (IVO24), which selectively targets the lung, breast, prostate, liver and oral cancer cells was conjugated to the nanocapsule surface. When tested *in vivo* against HeLa and MCF-7 cell lines, application of an alternating magnetic field (16 kA m^{-1}, 50 kHz, 2.5 min) on a drug-free nanocapsule was able to reduce cell viability to ~20% *via* magnetically induced hyperthermia; cell viability was further reduced to 2% when the alternating magnetic field was applied to nanocapsules containing both drugs. These promising results inspired further investigation *in vivo* wherein the magnetically triggered (8 kA m^{-1}, 50 kHz, 10 min at 24 h post injection)

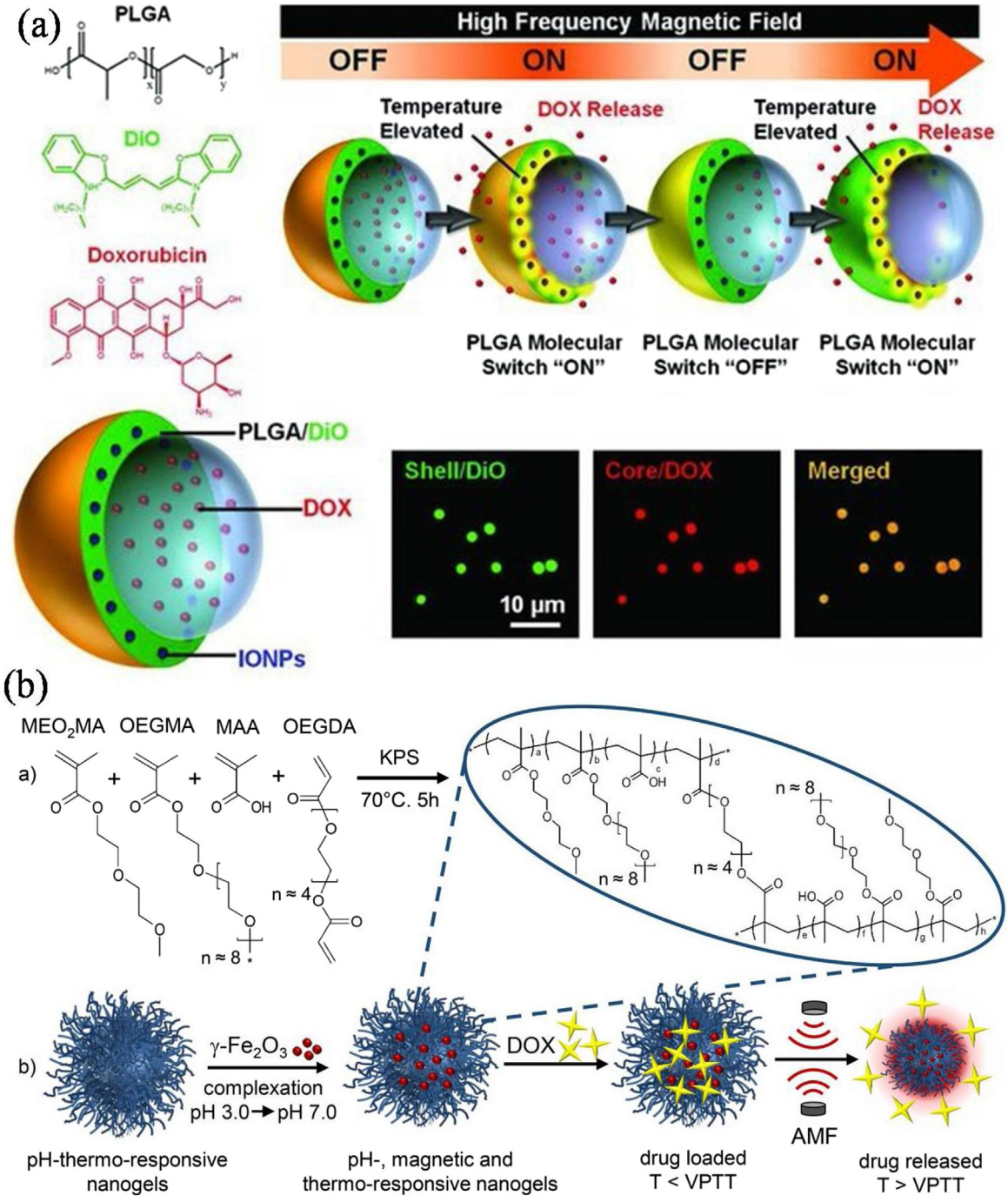

Fig. 11. (a) A schematic illustration of the structure and composition of smart hollow microspheres and its capability of pulsatile release in response to an externally applied magnetic field. [122], Copyright 2012. Reproduced with permission from WILEY-VCH Verlag GmbH & Co. KGaA, Weinheim. (b) Conventional aqueous precipitation radical copolymerization of nanogels based on oligo(ethylene glycol) methyl ether methacrylate monomers and illustration for the synthesis of magnetic nanogel and remotely controlled drug delivery under an alternating magnetic field. [127], Copyright 2017. Reproduced with permission from the American Chemical Society.

release of both drugs afforded near complete cessation of tumor growth. Zheng and co-workers self-assembled alternating layers of poly(allylamine hydrochloride) (PAH) and iron oxide nanoparticles from the surface of a $CaCO_3$ microparticles, which was subsequently removed to yield hollow polyelectrolyte microcapsules [125]. These multilayered microcapsules were loaded with insulin and were tested *in vitro*, where it was revealed that drug release only occurred upon application of an alternating magnetic field (50 kHz), hypothesized to occur due to enhanced membrane permeability. The drug release was observed to cease upon cessation of the applied magnetic field; this capability was used to demonstrate alternating cycles of drug release controlled by switching the alternating magnetic field between "ON" and "OFF" states. Lecommandoux and co-workers investigated the incorporation of ultrasmall superparamagnetic iron oxide nanoparticles (d = 9 nm) inside poly(trimethylene carbonate)-*b*-poly(L-glutamic acid) polymersomes for the remotely triggered intracellular delivery of doxorubicin [126]. The drug release was significantly increased when the synthesized polymersomes were exposed to a high frequency alternating magnetic field (14 mT, 750 kHz) when compared to the same polymersomes in the absence of a magnetic field. Ménager and co-workers reported the preparation of magnetore-

sponsive nanogels formed *via* the complexation of preformed iron oxide nanoparticles inside nanogels composed of oligo(ethylene glycol) (macro)monomers and methacrylic acid, with nanoparticle loadings as high as 66.7 wt% (Fig. 11b) [127]. The carboxyl moieties provided an additional pH sensitivity, affording complete release of loaded doxorubicin during a 4 h period when exposed to an alternating magnetic field (12 kA m^{-1}, 335 kHz, 30 min) under acidic conditions (pH = 5). More recently, Edirisinghe and co-workers reported the use of magnetic actuation, as opposed to the application of an alternating magnetic field, to facilitate drug release [128]. Citric acid coated iron oxide nanoparticles were mixed with poly(vinyl alcohol) and spun into fibers *via* an infusion gyration process. Acetaminophen, which was selected as a model drug, was loaded into the fibers by pressing with a spatula. Drug release was afforded by simply placing a commercial neodymium magnet against the glass wall containing the fiber sample; the magnetoresponsive fibers exhibited burst behavior wherein c.a. 70% of the loaded acetaminophen was released during the first 5 min. In contrast, samples that were not actuated with a magnet displayed negligible release during the same time frame. Chang and co-workers reported the fabrication of magnetoresponsive porous microparticles *via* electrospraying [129].

2.4. Electric field responsive systems

In addition to magnetic-responsive drug release, electric stimuli systems are also widely applied to achieve the spatially and temporally controlled drug release based on the conducting polymers or implantable electronic devices [55,130]. Conducting polymers such as polyaniline, polythiophene and polypyrrole and their various derivatives have been widely applied in neural prostheses, controlled release systems and neural probes [131]. Furthermore, electric fields can be easily applied to develop wireless dermal or implantable electronic delivery devices to achieve on demand drug release *via* the application of an external electric field of varying intensities [132,133]. As modern devices provide fine control over the voltage, a corresponding fine degree of control over the drug release may be realizable [132,162,163]. However, implantable electronic delivery devices often require invasive surgery [136]. Although electroresponsive systems provide significant advantages, a major obstacle may be the low penetration depth and the undesirable tissue damage that could arise at higher voltages [137] (Table 4).

Polymeric drug release nanocarriers potentially allows for release profiles that can be tailored to match physiological processes. The conductive polymer poly(pyrrole) (PPy) has been widely applied for controlled drug administration triggered by electrical stimulation. The good biocompatibility of this polymer makes it an ideal polymer for drug release applications. Langer's group developed an approach that relied on direct release from PPy with a broad range of payloads independent of molecular weight and charge [134]. By incorporating biotin as a dopant, electrical stimulation resulted in reduction of the PPy backbone, which was believed to trigger the release of biotin and the attached payload. A mass of compounds, biomolecules and drugs can be released utilizing the delivery of nerve growth factor (NGF) as a model system. NGF is a member of the neurotrophin family that influences neural growth, differentiation, survival and death in the central and peripheral nervous systems. Multiple compounds could be released by selectively attaching compounds to an array of PPy electrodes. This approach is especially compelling when used with degradable conductive polymers. Redenti and Langer cultured cells on an electroconductive transplantable polymer poly(pyrrole) and measured gene expression and morphology of the mouse retinal progenitor cells (mRPC) to simulate *in vitro* the spontaneous electrical wave activity associated with retinal development and investigate if such biometrically designed signals can enhance differentiation of cells [135]. The experimental evidence shows that the application of electrical stimulation on retinal development can be implemented to direct and enhance retinal differentiation of mRPCs, revealing a role for biomimetic electrical stimulation in directing progenitor cells toward neural fates.

Zare and co-workers reported the first *in vivo* demonstration of drug release triggered by an external electric field. Nanoparticles composed of the conductive polymer, poly(pyrrole), were prepared by emulsion polymerization, which also provided an avenue for drug encapsulation [136]. These conductive nanoparticles, measuring ~60 nm in diameter, were encapsulated inside thermoresponsive poly[d,l-lactic acid)-*co*-(glycolic acid)]-*b*-poly(ethylene oxide)-*b*-poly[(d,l-lactic acid)-*co*-(glycolic acid)] (PLGA-*b*-PEG-*b*-PLGA) block copolymers; these block copolymers could undergo a sol-gel transition where the polymer can transition from a liquid (~4 °C) to a hydrogel (~37 °C). Drug release was attributed to reduction/oxidation processes; reduction resulted in a less positive charge within the PPy nanoparticle and led to the repulsion-induced release of negatively charged fluorescein. Conversely, oxidation resulted in a more positive charge inside the PPy nanoparticles, causing the positively charged daunorubicin to be expelled. Following exit from the conductive nanoparticles, these molecules further exit the hydrogel towards the electrode bearing the opposite charge. This work demonstrated the potential of remotely triggering drug release *via* the application of an electric field and hints at the potential to selectively release co-loaded drug molecules by manipulating the nature of the electric field (reduction/oxidation).

Yuan and co-workers also utilized ferrocenyl motifs for the fabrication of voltage responsive vesicles capable of reversible self-assembly (Fig. 12a) [130]. The system consisted of a polystyrene chain end-capped with a β-cyclodextrin (β-CD) motif, which was paired with a poly(ethylene oxide) homopolymer containing a terminal ferrocenyl group; the uncharged ferrocene species binds strongly inside the β-CD, forming a "block copolymer" *in situ*. However, upon application of an oxidizing voltage (-1.5 V), the charged ferrocenyl cations are ejected from the β-CD cavity, resulting in the dissociation of the block conformation and its self-assembled structure as well. Application of a reductive voltage (-1.5 V), reverts the ferrocenyl functionality to its neutral state and therefore enables the host-guest induced self-assembly to proceed. Rhodamine B was encapsulated as a model species to demonstrate its on-demand release capability; release from the voltage responsive vesicles was a function of the applied voltage with higher oxidative potentials resulting in accelerated disassembly. Ren and co-workers reported the preparation of a novel voltage-responsive reversible self-assembly system (Fig. 12b) [138]. Poly(ethylene glycol)-*b*-poly(acrylic acid) (PEG_{113}-*b*-PAA_{30}) double hydrophilic block copolymers were self-assembled into micelles *via* the addition of a cationic ferrocenyl surfactant (11-ferrocenylundecyl) trimethylammonium bromide, FTMA. The key to this work was the reversible redox behavior of the ferrocene moiety; the ferrocenyl group can be oxidized into ferrocenium cations which disrupts the as formed micelles due to the increased hydrophilicity. This electrically induced disassembly process was demonstrated by the release of rhodamine 6 G, which was observed to increase in rate with increasing oxidative voltage *via* electrostatic attraction. Kim's group reported the fabrication of electric-field triggerable liposomes formed *via* anchoring poly(hydroxyethyl acrylate-*co*-hexadecyl acrylate-*co*-carboxyethyl acrylate) random copolymers onto the surface of phosphatidylcholine liposomes [139]. The application of an electric field ionizes the carboxyl functionalities of the anchored chain; the attraction of the anionic moieties to the anode induces shear stress on the liposomal membrane causing the release of encapsulated molecules. Additionally, H^+ produced

Table 4
Summary of electrically triggered drug release *in vivo*/*vitro*.

Ref. Year	Irradiation protocol	Electric-responsive system	Electric-responsive release mechanism	Therapeutic agents and dose
[131] 2018	0/1.0/3.0 V 3 min	Poly(chitosan-graft-polyaniline)/poly(oxidized dextran) injectable hydrogels	Electrochemical reduction and oxidation processes	Amoxicillin/ Ibuprofen 1.5 mg/mL
[139] 2018	0/1.5/3.0/4.5 V On(1 min)/off(3 min)	1,2-Diacyl-sn-glycero-3-phosphocholine@ P(HEA-HAD-CEA) liposomal	Anionic migrated to anode produced shear stress and acidification-induced contraction of polymer chains	1,2-Diacyl-sn-glycero-3-phosphocholine 100 mg/mL
[132] 2017	−0.5 V-5.0 V 1.5/3 min	Poly(3-hexylthiophene)/poly vinylalcohol	Switchable permeability of the poly(3-hexylthiophene) can tune its wettability *via* oxidation or reduction under a bias voltage	Rhodamine 6 G/Fuorescein sodium salt/ Evans blue 5 mg/mL
[138] 2015	0.3/0.5/1.0 V 480/270/ 150 min	PEG_{113}-*b*-PAA_{30}/FTMA	Electrochemical redox reactions medicate (dis)aggregation	Rhodamine 6 G 13 wt%
[142] 2014	10 V 1 min	Graphene/PMMA hydrogel	The deswelling of the macroporous hydrogel under the electric field	Doxorubicin 6 μCi in 6 mL
[141] 2013	5.0-15 V 5 min	PMMA/pristine multiwalled carbon nanotubes hydrogel	The alignment of carbon nanotubes towards the anode leading to partial gel matrix destruction	^{14}C-sucrose 3 μCi in 10 mL
[136] 2012	−1.5 V/cm 40 sec	PLGA-*b*-PEG-*b*-PLGA/PPy NPs	Electrochemical reduction/oxidation and electric-field-driven movement of charged molecules	Daunorubicin 0.6 mg/mL
[140] 2012	2.0/5.0/10/15 V 5 min	RGO-PVA hydrogel	Electro-osmosis and electrophoresis; the negatively charged RGO toward anode leads to the morphology change	Lidocaine hydrochloride 0.479 %

by the electrolysis of water could also induce compression within the liposomal membrane, providing a secondary pathway to membrane disruption. Release studies showed that encapsulated calcein released as function of both the carboxyl content present in the liposomes and also the applied voltage.

Yan and co-workers reported the fabrication of a voltage responsive device for remote controlled drug release (Fig. 13a) [132]. The device consisted of glass substrate patterned with an indium tin oxide (ITO) electrode that was then sequentially coated with thin films of polyvinyl alcohol and poly(3-hexylthiophene) respectively. The poly(3-hexylthiophene) layer played a critical role in this device whereby the application of low oxidative voltage (≈1 V) causes the conductive polymer to undergo a hydrophobic to hydrophilic transition. The enhanced permeability arising from this transition permits the release of encapsulated molecules. The authors demonstrated the versatility of the device by loading and releasing a wide range of molecules, which included fluorescent dyes and the anti-cancer drug, cisplatin. Furthermore, the low voltage requirements of the device enabled the authors to demonstrate the ability to switch the device between "ON" and "OFF" states wirelessly using a mobile phone, hinting at the great potential of this device. Guo and co-workers designed an electric field responsive injectable hydrogel by mixing chitosan-*g*-polyaniline with oxidized dextran (Fig. 13b) [131]. The authors investigated the release of hydrophilic amoxicillin and hydrophobic ibuprofen, wherein the application of an oxidative voltage (1 or 3 V) resulted in a pulsatile release that returned to the passive release rate upon switching off the voltage. The synthesized hydrogel with inherent antibacterial activity also exhibited excellent cytocompatibility, *in vivo* biocompatibility and biodegradability.

A voltage responsive hybrid hydrogel comprised of reduced graphene oxide (rGO) embedded in a matrix of poly(vinyl alcohol) was reported by Chen and co-workers [140]. The release of the local anesthetic, lidocaine hydrochloride, was investigated by passing an oxidative voltage (2–15 V) through the hydrogels which had rGO contents in the range of 8–44 wt%. Passive release rates, measured in the absence of an electric field, showed that the release of lidocaine decreased with increased rGO content. Application of an oxidative voltage reversed this trend with significant acceleration observed with increasing rGO content. Kostarelos and co-workers reported the preparation of electroresponsive hydrogels utilizing multiwalled carbon nanotubes (MWNT) [141] and graphene [142] as the conductive component. The hybrid hydrogels were prepared by the radical polymerization of methacrylic acid and *N*,*N*'-methylene bisacrylamide in the presence of an aqueous dispersion of either MWNTs or graphene; electrical stimulation of these hydrogels induces deswelling which results in the expulsion of water and loaded species. Comparison of the two *in vitro* and *in vivo* showed that under electrical stimulation (10 V, 5 min), radiolabelled sucrose ([^{14}C]-sucrose) was found to release from the graphene containing gel in greater amounts in a pulsatile fashion.

2.5. Ultrasound responsive systems

Ultrasound is predominantly used in a clinical setting as a diagnostic modality, providing real time images of blood flow [143–145]. Ultrasounds represent an effective and promising stimulus for achieving spatiotemporally controlled drug release at the desired location, avoiding harmful systemic effects. The use of ultrasound as a remote trigger for drug release has emerged as a promising strategy in biomedical applications in recent years, especially in tumor therapy [146–152]. Typically, ultrasound can be classified into low-frequency (20–100 kHz) and high-frequency (≥ 0.7 MHz); the differing capabilities may have a significant effect of the drug release behavior [153]. Ultrasound induces drug release *via* the generation of cavitation bubbles; the collapse of bubbles results in substantial mechanical and thermal effects which cause the destabilization of the drug nanocarrier. The enhanced tissue permeability further improves the drug release rate and induces cellular phagocytosis of the loaded therapeutic molecules or drugs [4] (Table 5).

Wang and co-workers designed curcumin encapsulated micelles composed of pluronic P123 and F127 polymers (Fig. 14a) [154]. Exposure to ultrasound resulted in curcumin release that was dependent on load power rather than duration, with the release rates decreasing significantly upon switching off the ultrasound. Application of this system *in vivo* revealed that the combination of curcumin encapsulated micelles stimulated by ultrasound provided the greatest tumor inhibition over 21 days; the enhanced efficacy in comparison to free curcumin (with and

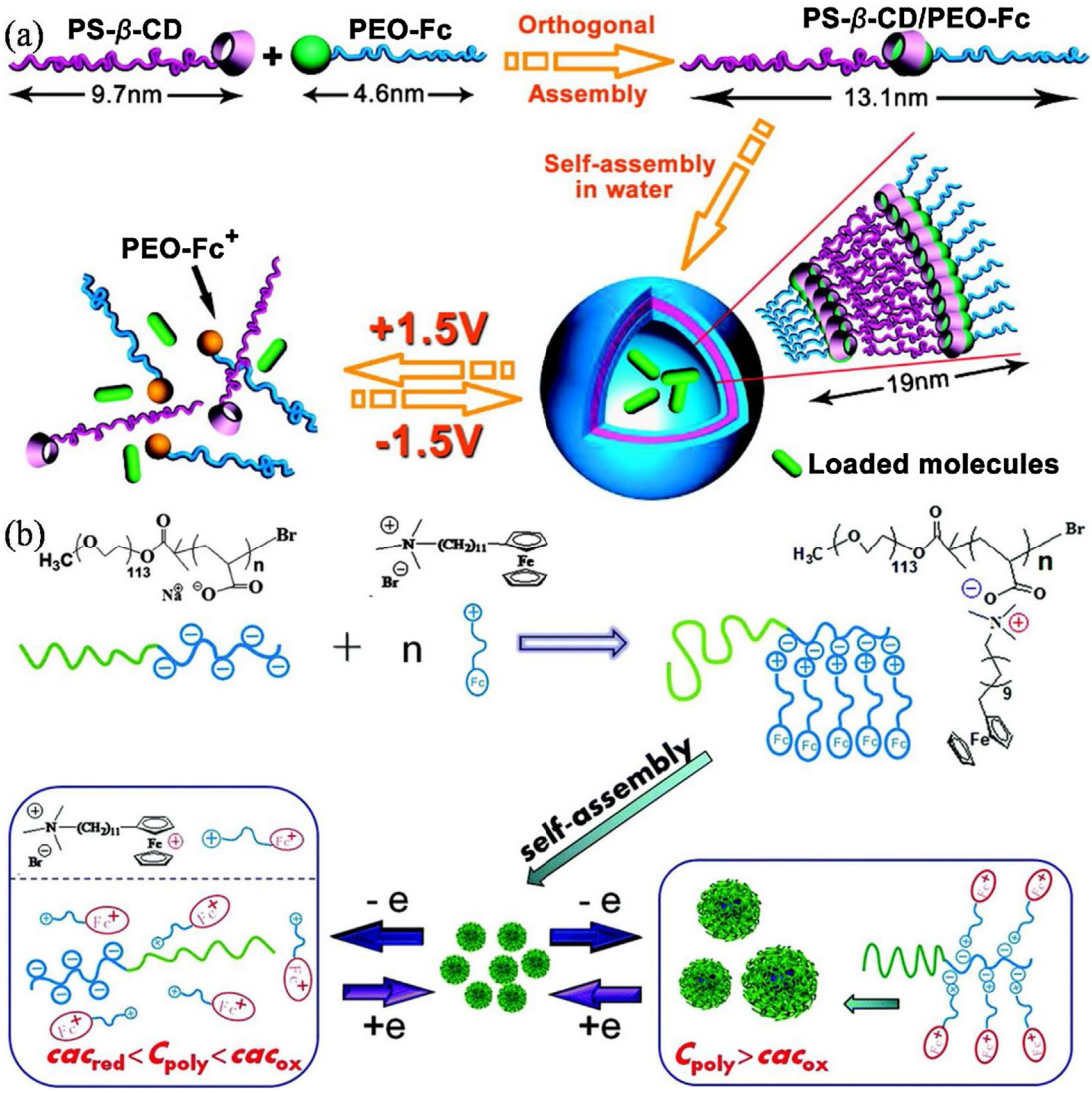

Fig. 12. (a) Structure of poly(styrene)-*β*-cyclodextrin (PS-*β*-CD) and poly(ethylene oxide)-ferrocene (PEO-Fc) as well as the voltage-responsive controlled assembly and disassembly of PS-*β*-CD/PEO-Fc vesicles. [130], Copyright 2010. Reproduced with permission from the American Chemical Society. (b) Schematic illustration for the voltage-responsive reversible aggregation behavior of the polymeric superamphiphile PEG_{113}-*b*-PAA_{30}/FTMA. [138], Copyright 2015. Reproduced with permission from the Royal Society of Chemistry.

Table 5
Summary of ultrasound (US) triggered drug release *in vivo*/*vitro*.

Ref. Year	Irradiation protocol	Ultrasound-responsive system	Ultrasound-responsive release mechanism	Therapeutic agents and dose
[157] 2017	1 MHz/20 kHz 1.0/1.5 MPa 2 min	PEG-*b*-PCL polymeric micelles	Perfluorocarbon core undergoes a liquid to gas phase transition under ultrasound	Propofol 177 μg/mL
[154] 2017	0.4 W/cm^2 3 min 1.0/1.9 MHz 1.0/2.0/3.0 W	Pluronic P123/F127 polymeric micelles encapsulating curcumin	US-induced cavitation and cavitation-induced sonoporation increase permeabilization and Us regulated self-assembly of micelles	Annexin V-FITC apoptosis detection kit and red fluorescent dye 1 mg/mL
[155] 2016	925 kHz 800 kPa 3 min	NH_2-PEG-NH_2/hyaluronic acid-hexadecylamine	HIFUS disintegrates the micelle structures and enhances permeability of the cell membrane	Docetaxel Anhydrou 10 μg/mL
[156] 2015	3 MHz 37 V 2 min PRF = 4 Hz	Gadoteridol@DOX liposomes	LINFUS induced sonoporation and permeabilization	Doxorubicin 1 mg/mL
[158] 2015	1.85 MHz 265 kPa 0-180 sec	PEG-human serum albumin@perfluoropentane@IONPs	Vaporization and cavitation-medicated sonoporation resulting shell swelling/cracking	Paclitaxel 0.5 μM
[159] 2015	1.3 MHz 100 W 5 min	P(MEO_2MA-*co*-THPMA)/mesoporous silica nanoparticles	Bond breaking under US resulting the hydrophobicity change	Fluorescein sodium salt/ $[Ru(bipy)_3]Cl_2$ 20 mg/mL
[160] 2013	40 kHz 360 W 37 °C 15 min	Polydimethylsiloxanemicrocapsules	US changes the porosity of the microcapsules in a nondestructive manner or destroy the walls	Domperidone maleate 340 μg/mL

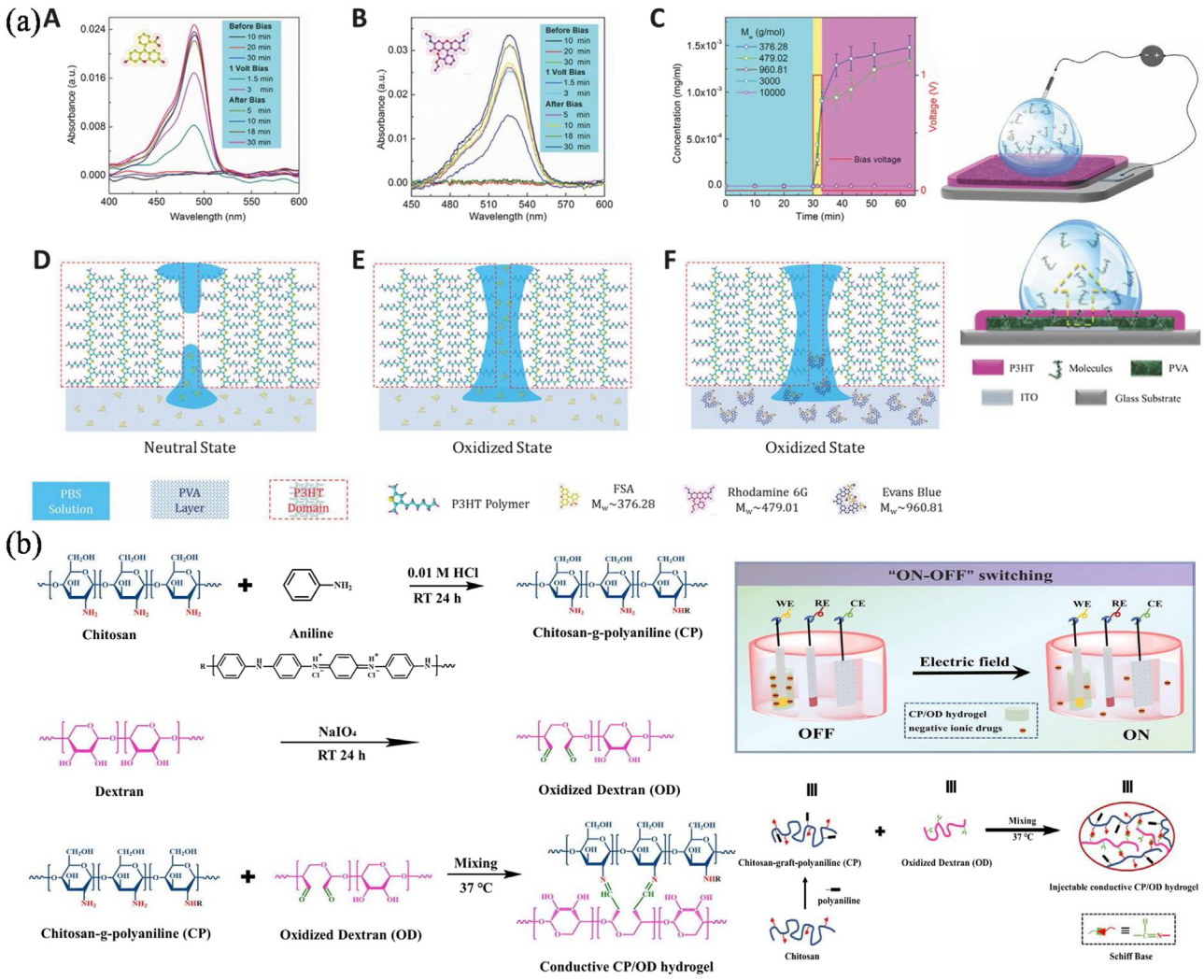

Fig. 13. (a) Schematic diagram of the drug release device based on conjugated polymer poly(3-hexylthiophene) and different molecules release from the organic devices controlled by a bias voltage. [132], Copyright 2017. Reproduced with permission from WILEY-VCH Verlag GmbH & Co. KGaA, Weinheim. (b) Schematic illustration for the synthesis of polymer CP/OD hydrogel and the pulse release of drug molecule from the CP/OD conductive polymer hydrogel. [131], Copyright 2018. Reproduced with permission from Elsevier Science Ltd.

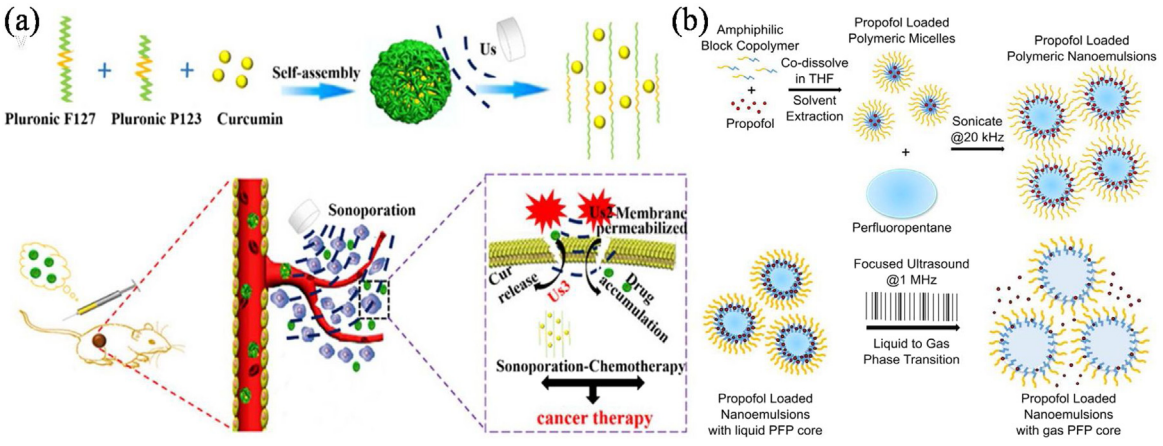

Fig. 14. (a) Schematic illustration for the preparation of Cur-M and ultrasound triggered drug release. [154], Copyright 2017. Reproduced with permission from the American Chemical Society. (b) Schematic for preparation and application of focused ultrasound-gated drug delivery nanoparticles. [157], Copyright 2017. Reproduced with permission from the American Chemical Society.

without ultrasonication) and curcumin loaded micelles that were not irradiated was attributed to the triggered drug release in combination with the increased vascular permeability afforded by application of ultrasound, the release rates decreased significantly. Park and co-workers prepared hyaluronic acid based micelles containing docetaxel and investigated their release when irradiated with high intensity focused ultrasound (925 kHz) [155]. *In vitro* drug release showed a pulsatile release behavior on application of the focused ultrasound and led to the reduced viability of CT-26 and MDA-MB-231 cells as a function of the loaded docetaxel content. Terreno and co-workers investigated the release of doxorubicin and the MRI contrast agent, Gadoteridol, that were encapsulated inside phospholipid-based liposomes [156]. Using pulsed low intensity non focused ultrasounds (pLINFU), release of both drugs were observed to be dependent on the pulse repetition frequency (PRF), with a PRF value of 2.5 Hz achieving the highest *in vitro* release. Additionally, no release was detected in the absence of ultrasound stimulation. *In vivo* experiments were carried out to confirm the theranostic performance on a syngeneic murine model of TS/A breast cancer. The results displayed the great potential of US-based stimuli to safely trigger the release of drug from the synthesized nanocarrier and significantly improve the therapeutic efficacy.

Green and co-workers utilized the liquid to gas phase transition of perfluorcarbons as an ultrasound responsive trigger (Fig. 14b) [157]. Poly(ethylene glycol)-*b*-polycaprolactone amphiphilic block copolymers were micellized in the presence of propofol and subsequently sonicated (20 kHz) in the presence of liquid perfluoropentane to produce a sonoresponsive nanoemulsion. The system was then studied *in vivo* wherein focused ultrasound (1 MHz) was successfully used to induce the release of propofol and subsequent silencing of seizure activity. Perfluoropentane loaded nanodroplets were reported by Stride and co-workers as a sono-triggerable drug delivery vehicle [158]. The nanodroplet was stabilized inside a crosslinker shell composed of human serum albumin and poly(ethylene glycol) and was co-loaded with paclitaxel and iron oxide nanoparticles. Continuous wave ultrasound irradiation (1.85 MHz) induced the gasification of the perfluoropentane core; a key finding was that the co-loaded iron oxide nanoparticles, hypothesized to have been acting as nucleation agents, enhanced the vaporization process. Vallet-Regi and co-workers reported a novel strategy for designing ultrasound triggerable drug delivery systems [159]. The key to this work was the use of the monomer, 2-tetrahydropyranyl methacrylate (THPMA); the monomer can undergo a hydrophobic to hydrophilic transition *via* ultrasound induced cleavage of its labile acetal group, leading to its transformation into methacrylic acid. The authors copolymerized THPMA with a thermoresponsive monomer, 2-(2-methoxyethoxy)ethyl methacrylate, which was conjugated onto the surface of mesoporous silica nanoparticles. At 4 °C, the copolymers were below their LCST and provided facile loading of fluorescein; upon warming to physiological temperature (37 °C), the copolymers proceeded to undergo an LCST transition to a coil-like conformation which effectively blocked the pores, impeding cargo release. Ultrasonic irradiation (1.3 MHz, 100 W) of these hybrid nanoparticles for 10 min elicited a burst release response wherein > 70% of the loaded fluorescein was released in the first 5 h and was followed by a decreasing rate.

Zhou and co-workers reported the preparation of polydimethylsiloxane hollow microcapsules for sonoresponsive drug release [160]. The microfluidic fabrication method utilized in their work enabled the formation of both eccentric and core-centered inner cavities; under ultrasound irradiation (40 kHz, 360 W), the eccentric microcapsules exhibited a significantly higher release rate in comparison to their centered counterparts, which could be explained by the differences in their shell thicknesses (c.a. 130 nm *vs* 8 nm). Shimizu and co-workers reported the preparation of liposomes composed of pegylated phospholipids and a thermoresponsive copolymer, P(*N*-isopropylmethacrylamide-*co*-*N*-isopropylacrylamide) [poly(NIPMAM-*co*-NIPAM)], which was further decorated with single stranded DNA aptamers as targeting ligands [161]. Ultrasound irradiation (1 MHz, 0.5 W cm^{-1}, 30 s) of calcein loaded liposomes were observed to release above 60% of their payload; the release of calcein was facilitated not by an increase in bulk temperature but due to localized heating arising from the collapse of cavitation bubbles.

3. Conclusions and outlook

The constructed nanocarriers responsive to the exogenous or endogenous stimuli are developing into a promising strategy. This minireview briefly elucidates the exciting research progress on polymer systems responsive to light, microwave, magnetic field, electric field and ultrasound stimuli for remotely controlled drug release. Remote triggering provides consistent, on-demand dosing, with reduced systemic toxicity that coincides with increased treatment efficacy. The design of stimuli-responsive polymer systems and formulations for remotely controlled drug molecule release are highlighted in particular. These advances should result from the convergence of chemical and physical properties of the stimuli-responsive functional polymers, which plays an important role in the development of theranostic systems. Multifunctional polymer systems which have the functions of targeting and tracking for drug molecules are currently under active development to facilitate more efficient treatments.

Despite advancements in this field, great challenges still exist and need to be addressed. For instance, bio-safety is one of the most important factors for nanomaterials which are utilized in biomedical fields and should be comprehensively assessed before the final clinical application. However, knowledge concerned with the toxicity of various carrier-materials is still very limited. Furthermore, the accumulation of material, inert or otherwise, is serious long-term concern highly relevant to the design and implementation of any nanomaterials. To overcome these drawbacks, the development of cleavable or decomposable stimuli-responsive functional polymer systems for renal clearance is a promising strategy and in urgent demand. Additionally, the clearance pathways of the biodegradable polymers should be paid extensive attention and investigation. Further understanding on the detailed biodegradation mechanisms and toxicity assessments in body are still in early stage and needed to be explored. On the other hand, it is very difficult to confirm which stimuli-responsive polymer systems have the best opportunity to reach the clinic. Although various unsolved issues still remain, the promising potential of stimuli-responsive functional polymer systems for biomedical applications is undeniable. As discussed above, although the relevant research about remotely controlled drug delivery and release are still in its nascent stage, biomedical applications of stimuli-responsive polymer systems have attracted enormous research interests and experienced an extremely rapid growth over the past few years. We anticipate the design and development of more advanced stimuli-responsive polymer systems for biomedical applications in the near future.

Acknowledgements

This work was supported by Qingdao Innovation Leading Talent Program, Natural Science Foundation of Shandong (ZR2017BEM028).

References

[1] Emilio P, Jacqueline F, Meir B. Development of new antiepileptic drugs: challenges, incentives, and recent advances. Lancet Neurol 2007;6:793–804.
[2] Pollard JR, French J. Antiepileptic drugs in development. Lancet Neurol 2006;5:1064–7.
[3] Link H, Martin R. New drugs may improve, complicate treatment for multiple sclerosis. Nat Med 2010;16, 272-2.
[4] Mura S, Nicolas J, Couvreur P. Stimuli-responsive nanocarriers for drug delivery. Nat Mater 2013;12:991–1003.
[5] Zhou X, Chen L, Nie W, Wang W, Qin M, Mo X, et al. Dual-responsive mesoporous silica nanoparticles mediated codelivery of doxorubicin and Bcl-2 sirna for targeted treatment of breast cancer. J Phys Chem C 2016;120:22375–87.
[6] Shen S, Chao Y, Dong Z, Wang G, Yi X, Song G, et al. Bottom-up preparation of uniform ultrathin rhenium disulfide nanosheets for image-guided photothermal radiotherapy. Adv Funct Mater 2017;27(1700250):1–9.
[7] Zhu H, Lai Z, Fang Y, Zhen X, Tan C, Qi X, et al. Ternary chalcogenide nanosheets with ultrahigh photothermal conversion efficiency for photoacoustic theranostics. Small 2017;13(1604139):1–9.
[8] Jia X, Bai J, Ma Z, Jiang X. BSA-exfoliated WSe2 nanosheets as a photoregulated carrier for synergistic photodynamic/photothermal therapy. J Mater Chem B 2017;5:269–78.
[9] Song G, Hao J, Liang C, Liu T, Gao M, Cheng L, et al. Degradable molybdenum oxide nanosheets with rapid clearance and efficient tumor homing capabilities as a therapeutic nanoplatform. Angew Chem Int Ed Engl 2016;55:2122–6.
[10] Kapil N, Singh A, Singh M, Das D. Efficient MoS_2 exfoliation by cross-beta-amyloid nanotubes for multistimuli-responsive and biodegradable aqueous dispersions. Angew Chem Int Ed Engl 2016;55:7772–6.
[11] Meng X, Liu Z, Cao Y, Dai W, Zhang K, Dong H, et al. Fabricating aptamer-conjugated pegylated-MoS_2/$Cu_{1.8}S$ theranostic nanoplatform for multiplexed imaging diagnosis and chemo-photothermal therapy of cancer. Adv Funct Mater 2017;27(1605592):1–10.
[12] Nguyen TK, Selvanayagam R, Ho KK, Chen R, Kutty SK, Rice SA, et al. Co-delivery of nitric oxide and antibiotic using polymeric nanoparticles. Chem Sci 2016;7:1016–27.
[13] Mishra D, Hubenak JR, Mathur AB. Nanoparticle systems as tools to improve drug delivery and therapeutic efficacy. J Biomed Mater Res A 2013;101:3646–60.
[14] Ma Y, Huang J, Song S, Chen H, Zhang Z. Cancer-targeted nanotheranostics: recent advances and perspectives. Small 2016;12:4936–54.
[15] Merino S, Martín C, Kostarelos K, Prato M, Vázquez E. Nanocomposite hydrogels: 3D polymer-nanoparticle synergies for on-demand drug delivery. ACS Nano 2015;9:4686–97.
[16] Shi Y, Liu M, Deng F, Zeng G, Wan Q, Zhang X, et al. Recent progress and development on polymeric nanomaterials for photothermal therapy: a brief overview. J Mater Chem B 2017;5:194–206.
[17] Meng Z, Wei F, Wang R, Xia M, Chen Z, Wang H, et al. NIR-laser-switched in vivo smart nanocapsules for synergic photothermal and chemotherapy of tumors. Adv Mater 2016;28:245–53.
[18] Park CH, Yun H, Yang H, Lee J, Kim BJ. Fluorescent block copolymer-MoS_2 nanocomposites for real-time photothermal heating and imaging. Adv Funct Mater 2017;27(1604403):1–7.
[19] Zhang C, Yong Y, Song L, Dong X, Zhang X, Liu X, et al. Multifunctional WS_2 @poly(ethylene imine) nanoplatforms for imaging guided gene-photothermal synergistic therapy of cancer. Adv Healthc Mater 2016;5:2776–87.
[20] Lee J, Kim J, Kim WJ. Photothermally controllable cytosolic drug delivery based on core-shell MoS_2-porous silica nanoplates. Chem Mater 2016;28:6417–24.
[21] Zhao L, Yuan W, Tham HP, Chen H, Xing P, Xiang H, et al. Fast-clearable nanocarriers conducting chemo/photothermal combination therapy to inhibit recurrence of malignant tumors. Small 2017;13(1700963):1–9.
[22] Liu L, Wang J, Tan X, Pang X, You Q, Sun Q, et al. Photosensitizer loaded PEG-MoS_2-Au hybrids for CT/NIRF imaging-guided stepwise photothermal and photodynamic therapy. J Mater Chem B 2017;5:2286–96.
[23] Zhang L, Chen Y, Li Z, Li L, Saint-Cricq P, Li C, et al. Tailored synthesis of octopus-type janus nanoparticles for synergistic actively-targeted and chemo-photothermal therapy. Angew Chem Int Ed Engl 2016;55:2118–21.
[24] Yu J, Yin W, Zheng X, Tian G, Zhang X, Bao T, et al. Smart MoS_2/Fe_3O_4 nanotheranostic for magnetically targeted photothermal therapy guided by magnetic resonance/photoacoustic imaging. Theranostics 2015;5:931–45.
[25] Li A, Zhang J, Xu Y, Liu J, Feng S. Thermoresponsive copolymer/SiO_2 nanoparticles with dual functions of thermally controlled drug release and simultaneous carrier decomposition. Chem Eur J 2014;20:12945–53.
[26] K CR, Thapa B, Xu P. PH and redox dual responsive nanoparticle for nuclear targeted drug delivery. Mol Pharm 2012;9:2719–29.
[27] Feng W, Chen L, Qin M, Zhou X, Zhang Q, Miao Y, et al. Flower-like PEGylated MoS_2 nanoflakes for near-infrared photothermal cancer therapy. Sci Rep 2015;5(17422):1–13.
[28] Wei M, Gao Y, Li X, Serpe MJ. Stimuli-responsive polymers and their applications. Polym Chem 2017;8:127–43.
[29] Yin W, Yu J, Lv F, Yan L, Zheng LR, Gu Z, et al. Functionalized nano-MoS_2 with peroxidase catalytic and near-infrared photothermal activities for safe and synergetic wound antibacterial applications. ACS Nano 2016;10:11000–11.
[30] Zhou SM, Ma DK, Zhang SH, Wang W, Chen W, Huang SM, et al. Pegylated Cu_3BiS_3 hollow nanospheres as a new photothermal agent for 980 nm-laser-driven photothermochemotherapy and a contrast agent for x-ray computed tomography imaging. Nanoscale 2015;8:1374–82.
[31] Song G, Liang C, Gong H, Li M, Zheng X, Cheng L, et al. Core-shell MnSe@Bi_2Se_3 fabricated via a cation exchange method as novel nanotheranostics for multimodal imaging and synergistic thermoradiotherapy. Adv Mater 2015;27:6110–7.
[32] Zhang A, Li A, Zhao W, Yan G, Liu B, Liu M, et al. An efficient and self-guided chemo-photothermal drug loading system based on copolymer and transferrin decorated MoS_2 nanodots for dually controlled drug release. Chem Eng J 2018;342:120–32.
[33] Timko BP, Dvir T, Kohane DS. Remotely triggerable drug delivery systems. Adv Mater 2010;22:4925–43.
[34] Chen L, Feng Y, Zhou X, Zhang Q, Nie W, Wang W, et al. One-pot synthesis of MoS_2 nanoflakes with desirable degradability for photothermal cancer therapy. ACS Appl Mater Interfaces 2017;9:17347–58.
[35] Liu Q, Zhan C, Kohane DS. Phototriggered drug delivery using inorganic nanomaterials. Bioconjug Chem 2017;28:98–104.
[36] Shen S, Liu M, Li T, Lin S, Mo R. Recent progress in nanomedicine-based combination cancer therapy using a site-specific co-delivery strategy. Biomater Sci 2017;5:1367–81.
[37] Lim EK, Kim T, Paik S, Haam S, Huh YM, Lee K. Nanomaterials for theranostics: recent advances and future challenges. Chem Rev 2015;115:327–94.
[38] Li X, Shan J, Zhang W, Su S, Yuwen L, Wang L. Recent advances in synthesis and biomedical applications of two-dimensional transition metal dichalcogenide nanosheets. Small 2017;13(1602660):1–28.
[39] Xue F, Wen Y, Wei P, Gao Y, Zhou Z, Xiao S, et al. A smart drug: a pH-responsive photothermal ablation agent for golgi apparatus activated cancer therapy. Chem Commun 2017;53:6424–7.
[40] Qin Y, Chen J, Bi Y, Xu X, Zhou H, Gao J, et al. Near-infrared light remote-controlled intracellular anti-cancer drug delivery using thermo/pH sensitive nanovehicle. Acta Biomater 2015;17:201–9.
[41] Hervault A, Dunn AE, Lim M, Boyer C, Mott D, Maenosono S, et al. Doxorubicin loaded dual pH- and thermo-responsive magnetic nanocarrier for combined magnetic hyperthermia and targeted controlled drug delivery applications. Nanoscale 2016;8:12152–61.
[42] Dunn AE, Dunn DJ, Macmillan A, Whan R, Stait-Gardner T, Price WS, et al. Spatial and temporal control of drug release through pH and alternating magnetic field induced breakage of schiff base bonds. Polym Chem 2014;5:3311–5.
[43] Quan F, Zhang A, Cheng F, Cui L, Liu J, Xia Y. Biodegradable polymeric architectures via reversible deactivation radical polymerizations. Polymers 2018;10(758):1–26.
[44] Cai Z, Zhang H, Wei Y, Cong F. Hyaluronan-inorganic nanohybrid materials for biomedical applications. Biomacromolecules 2017;18:1677–96.
[45] Elman NM, Masi BC, Cima MJ, Langer R. Electro-thermally induced structural failure actuator (ETISFA) for implantable controlled drug delivery devices based on micro-electro-mechanical-systems. Lab Chip 2010;10:2796–804.
[46] Bertrand O, Gohy JF. Photo-responsive polymers: synthesis and applications. Polym Chem 2017;8:52–73.
[47] Bagheri A, Yeow J, Arandiyan H, Xu J, Boyer C, Lim M. Polymerization of a photocleavable monomer using visible light. Macromol Rapid Commun 2016;37:905–10.
[48] Li Y, Liu G, Ma J, Lin J, Lin H, Su G, et al. Chemotherapeutic drug-photothermal agent co-self-assembling nanoparticles for near-infrared fluorescence and photoacoustic dual-modal imaging-guided chemo-photothermal synergistic therapy. J Control Release 2017;258:95–107.
[49] Yin W, Yan L, Yu J, Tian G, Zhou L, Zheng X, et al. High-throughput synthesis of single-layer MoS_2 nanosheets as a near-infrared photothermal-triggered drug delivery for effective cancer therapy. ACS Nano 2014;8:6922–33.
[50] Kamaly N, Yameen B, Wu J, Farokhzad OC. Degradable controlled-release polymers and polymeric nanoparticles: mechanisms of controlling drug release. Chem Rev 2016;116:2602–63.
[51] Liu X, Xu JF, Wang Z, Zhang X. Photo-responsive supramolecular polymers synthesized by olefin metathesis polymerization from supramonomers. Polym Chem 2016;7:2333–6.
[52] Goel S, Chen F, Cai W. Synthesis and biomedical applications of copper sulfide nanoparticles: from sensors to theranostics. Small 2014;10:631–45.
[53] Marturano V, Bizzarro V, De Luise A, Calarco A, Ambrogi V, Giamberini M, et al. Essential oils as solvents and core materials for the preparation of photo-responsive polymer nanocapsules. Nano Res 2018;11:2783–95.
[54] Grayson ACR, Choi IS, Tyler BM, Wang PP, Brem H, Cima MJ, et al. Multi-pulse drug delivery from a resorbable polymeric microchip device. Nat Mater 2003;2:767–72.
[55] Li L, Wu Y, Du FS Li ZC. Modular synthesis of photodegradable polymers with different sensitive wavelengths as UV/NIR responsive nanocarriers. J Polym Sci Part A Polym Chem 2019;57:334–41.
[56] Joglekar M, Trewyn BG. Polymer-based stimuli-responsive nanosystems for biomedical applications. Biotechnol J 2013;8:931–45.

[57] Hang C, Zou Y, Zhong Y, Zhong Z, Meng F. NIR and UV-responsive degradable hyaluronic acid nanogels for CD44-targeted and remotely triggered intracellular doxorubicin delivery. Colloids Surf B 2017;158:547–55.
[58] Li Q, Li W, Di H, Luo L, Zhu C, Yang J, et al. A photosensitive liposome with nir light triggered doxorubicin release as a combined photodynamic-chemo therapy system. J Control Release 2018;277:114–25.
[59] Dou R, Du Z, Bao T, Dong X, Zheng X, Yu M, et al. The polyvinylpyrrolidone functionalized rGO/Bi_2S_3 nanocomposite as a near-infrared light-responsive nanovehicle for chemo-photothermal therapy of cancer. Nanoscale 2016;8:11531–42.
[60] Shanmugam S, Xu J, Boyer C. Light-regulated polymerization under near-infrared/far-red irradiation catalyzed by bacteriochlorophyll a. Angew Chem Int Ed Engl 2016;55:1036–40.
[61] Zhang A, Li A, Tian W, Li Z, Wei C, Sun Y, et al. A target-directed chemo-photothermal system based on transferrin and copolymer-modified MoS_2 nanoplates with pH-activated drug release. Chem Eur J 2017;23:11346–56.
[62] Li H, Yang X, Zhou Z, Wang K, Li C, Qiao H, et al. Near-infrared light-triggered drug release from a multiple lipid carrier complex using an all-in-one strategy. J Control Release 2017;261:126–37.
[63] Park JH, Choi JH, Son JH, Hwang SJ, Seo H, Kang IK, et al. Poly(ε-caprolactone) (PCL) fibers incorporated with phase-changeable fatty acid and indocyanine green for nir light-triggered, localized anti-cancer drug release. Polymer 2018;135:211–8.
[64] Wang P, Chen S, Cao Z, Wang G. Nir light-, temperature-, pH-, and redox-responsive polymer-modified reduced graphene oxide/mesoporous silica sandwich-like nanocomposites for controlled release. ACS Appl Mater Interfaces 2017;9:29055–62.
[65] Keurentjes J, Kemmere M, Bruinewoud H, Vertommen M, Rovers S, Hoogenboom R, et al. Externally triggered glass transition switch for localized on-demand drug delivery. Angew Chem Int Ed Engl 2009;48:9867–70.
[66] Wang Y, Li S, Zhang P, Bai H, Feng L, Lv F, et al. Photothermal-responsive conjugated polymer nanoparticles for remote control of gene expression in living cells. Adv Mater 2018;30(1705418):1–5.
[67] Zhang A, Li A, Zhao W, Liu J. Recent advances in functional polymer decorated two-dimensional transition-metal dichalcogenides nanomaterials for chemo-photothermal therapy. Chem Eur J 2018;24:4215–27.
[68] Li Q, Cao Z, Wang G. Diazonaphthoquinone-based amphiphilic polymer assemblies for NIR/UV light-and pH-responsive controlled release. Polym Chem 2018;9:463–71.
[69] Tiwari AP, Hwang TI, Oh JM, Maharjan B, Chun S, Kim BS, et al. PH/NIR-responsive polypyrrole-functionalized fibrous localized drug-delivery platform for synergistic cancer therapy. ACS Appl Mater Interfaces 2018;10:20256–70.
[70] Deng Y, Käfer F, Chen T, Jin Q, Ji J, Agarwal S. Let there be light: polymeric micelles with upper critical solution temperature as light-triggered heat nanogenerators for combating drug-resistant cancer. Small 2018;14(1802420):1–10.
[71] Wu Y, Wang H, Gao F, Xu Z, Dai F, Liu W. An injectable supramolecular polymer nanocomposite hydrogel for prevention of breast cancer recurrence with theranostic and mammoplastic functions. Adv Funct Mater 2018;28(1801000):1–12.
[72] Li M, Sun X, Zhang N, Wang W, Yang Y, Jia H, et al. NIR-activated polydopamine-coated carrier-free "nanobomb" for in situ on-demand drug release. Adv Sci 2018;5(1800155):1–10.
[73] Cao J, Huang S, Chen Y, Li S, Li X, Deng D, et al. Near-infrared light-triggered micelles for fast controlled drug release in deep tissue. Biomaterials 2013;34:6272–83.
[74] Wang H, Ke F, Mararenko A, Wei Z, Banerjee P, Zhou S. Responsive polymer-fluorescent carbon nanoparticle hybrid nanogels for optical temperature sensing, near-infrared light-responsive drug release, and tumor cell imaging. Nanoscale 2014;6:7443–52.
[75] Shao J, Xuan M, Si T, Dai L, He Q. Biointerfacing polymeric microcapsules for in vivo near-infrared light-triggered drug release. Nanoscale 2015;7:19092–8.
[76] Salma SA, Patil MP, Kim DW, Le CMQ Ahn BH, Kim GD, et al. Near-infrared light-responsive, diselenide containing core-cross-linked micelles prepared by the diels–alder click reaction for photocontrollable drug release application. Polym Chem 2018;9:4813–23.
[77] Yu H, Cui Z, Yu P, Guo C, Feng B, Jiang T, et al. PH-and NIR light-responsive micelles with hyperthermia-triggered tumor penetration and cytoplasm drug release to reverse doxorubicin resistance in breast cancer. Adv Funct Mater 2015;25:2489–500.
[78] Wang X, Hu J, Liu G, Tian J, Wang H, Gong M, et al. Reversibly switching bilayer permeability and release modules of photochromic polymersomes stabilized by cooperative noncovalent interactions. J Am Chem Soc 2015;137:15262–75.
[79] Sun Z, Liu G, Hu J, Liu S. Photo-and reduction-responsive polymersomes for programmed release of small and macromolecular payloads. Biomacromolecules 2018;19:2071–81.
[80] Senthilkumar T, Zhou L, Gu Q, Liu L, Lv F, Wang S. Conjugated polymer nanoparticles with appended photo-responsive units for controlled drug delivery, release, and imaging. Angew Chem Int Ed Engl 2018;57:13114–9.
[81] Liu G, Wang X, Hu J, Zhang G, Liu S. Self-immolative polymersomes for high-efficiency triggered release and programmed enzymatic reactions. J Am Chem Soc 2014;136:7492–7.
[82] Carling CJ, Viger ML, Huu VAN, Garcia AV, Almutairi A. In vivo visible light-triggered drug release from an implanted depot. Chem Sci 2015;6:335–41.
[83] Truong VX, Li F, Forsythe JS. Photolabile hydrogels responsive to broad spectrum visible light for selective cell release. ACS Appl Mater Interfaces 2017;9:32441–5.
[84] Saravanakumar G, Lee J, Kim J, Kim WJ. Visible light-induced singlet oxygen-mediated intracellular disassembly of polymeric micelles co-loaded with a photosensitizer and an anticancer drug for enhanced photodynamic therapy. Chem Commun 2015;51:9995–8.
[85] Yeh HP, del Valle AC, Syu MC, Qian Y, Chang YC, Huang YF. A new photosensitized oxidation-responsive nanoplatform for controlled drug release and photodynamic cancer therapy. ACS Appl Mater Interfaces 2018;10:21160–72.
[86] Barhoumi A, Liu Q, Kohane DS. Ultraviolet light-mediated drug delivery: principles, applications, and challenges. J Control Release 2015;219:31–42.
[87] Wang X, Liu G, Hu J, Zhang G, Liu S. Concurrent block copolymer polymersome stabilization and bilayer permeabilization by stimuli-regulated "traceless" crosslinking. Angew Chem Int Ed Engl 2014;53:3138–42.
[88] Yuan W, Gao X, Pei E, Li Z. Light-and ph-dually responsive dendrimer-star copolymer containing spiropyran groups: synthesis, self-assembly and controlled drug release. Polym Chem 2018;9:3651–61.
[89] Li JY, Qiu L, Xu XF, Pan CY, Hong CY, Zhang WJ. Photo-responsive camptothecin-based polymeric prodrug coated silver nanoparticles for drug release behaviour tracking via the nanomaterial surface energy transfer (NSET) effect. J Mater Chem B 2018;6:1678–87.
[90] Zhang WM, Zhang J, Qiao Z, Liu HY, Wu ZQ, Yin J. Facile fabrication of positively-charged helical poly (phenyl isocyanide) modified multi-stimuli-responsive nanoassembly capable of high efficiency cell-penetrating, ratiometric fluorescence imaging, and rapid intracellular drug release. Polym Chem 2018;9:4233–42.
[91] Chen S, Bian Q, Wang P, Zheng X, Lv L, Dang Z, et al. Photo, pH and redox multi-responsive nanogels for drug delivery and fluorescence cell imaging. Polym Chem 2017;8:6150–257.
[92] Chen S, Jiang F, Cao Z, Wang G, Dang ZM. Photo, pH, and thermo triple-responsive spiropyran-based copolymer nanoparticles for controlled release. Chem Commun 2015;51:12633–6.
[93] Hu C, Ma N, Li F, Fang Y, Liu Y, Zhao L, et al. Cucurbit [8] uril-based giant supramolecular vesicles: highly stable, versatile carriers for photoresponsive and targeted drug delivery. ACS Appl Mater Interfaces 2018;10:4603–13.
[94] Chi X, Ji X, Xia D, Huang F. A dual-responsive supra-amphiphilic polypseudorotaxane constructed from a water-soluble pillar[7]arene and an azobenzene-containing random copolymer. J Am Chem Soc 2015;137:1440–3.
[95] Greco CT, Andrechak JC, Epps IIITH, Sullivan MO. Anionic polymer and quantum dot excipients to facilitate sirna release and self-reporting of disassembly in stimuli-responsive nanocarrier formulations. Biomacromolecules 2017;18:1814–24.
[96] Fan B, Gillies ER. Poly (ethyl glyoxylate)-poly (ethylene oxide) nanoparticles: stimuli-responsive drug release via end-to-end polyglyoxylate depolymerization. Mol Pharm 2017;14:2548–59.
[97] Huu VAN, Luo J, Zhu J, Zhu J, Patel S, Boone A, et al. Light-responsive nanoparticle depot to control release of a small molecule angiogenesis inhibitor in the posterior segment of the eye. J Control Release 2015;200:71–7.
[98] Fomina N, McFearin C, Sermsakdi M, Edigin O, Almutairi A. UV and NIR triggered release from polymeric nanoparticles. J Am Chem Soc 2010;132:9540–2.
[99] Son S, Shin E, Kim BS. Light-responsive micelles of spiropyran initiated hyperbranched polyglycerol for smart drug delivery. Biomacromolecules 2014;15:628–34.
[100] Wong T. Use of microwave in processing of drug delivery systems. Curr Drug Deliv 2008;5:77–84.
[101] Anuar NK, Wong TW, Taib MN. Microwave modified non-crosslinked pectin films with modulated drug release. Pharm Dev Technol 2012;17:110–7.
[102] Shi Y, Ma C, Du Y, Yu G. Microwave-responsive polymeric core-shell microcarriers for high-efficiency controlled drug release. J Mater Chem B 2017;5:3541–9.
[103] Qiu H, Cui B, Zhao W, Chen P, Peng H, Wang Y. A novel microwave stimulus remote controlled anticancer drug release system based on $Fe3O_4$@ZnO@ mGd_2O3:Eu@P(NIPAm-co-MAA) multifunctional nanocarriers. J Mater Chem B 2015;3:6919–27.
[104] Jin Y, Liang X, An Y, Dai Z. Microwave-triggered smart drug release from liposomes co-encapsulating doxorubicin and salt for local combined hyperthermia and chemotherapy of cancer. Bioconjug Chem 2016;27:2931–42.
[105] Hervault A, Dunn AE, Lim M, Boyer C, Mott D, Maenosono S, et al. Doxorubicin loaded dual pH- and thermo-responsive magnetic nanocarrier for combined magnetic hyperthermia and targeted controlled drug delivery applications. Nanoscale 2016;8:12152–61.

[106] Boyer C, Whittaker MR, Bulmus V, Liu J, Davis TP. The design and utility of polymer-stabilized iron-oxide nanoparticles for nanomedicine applications. NPG Asia Mater 2010;2:23–30.
[107] Mertz D, Sandre O, Begin-Colin S. Drug releasing nanoplatforms activated by alternating magnetic fields. Biochim Biophys Acta Gen Subj 2017;1861:1617–41.
[108] N'Guyen TT, Duong HT, Basuki J, Montembault V, Pascual S, Guibert C, et al. Functional iron oxide magnetic nanoparticles with hyperthermia-induced drug release ability by using a combination of orthogonal click reactions. Angew Chem Int Ed Engl 2013;52:14152–6.
[109] Rovers S, Kemmere M, Keurentjes J, Hoogenboom R. Repetitive on-demand drug release from polymeric matrices containing a macroscopic spherical iron core. J Mater Sci: Mater Med 2017;28:163.
[110] Massoumi B, Mozaffari Z, Jaymand M. A starch-based stimuli-responsive magnetite nanohydrogel as de novo drug delivery system. Int J Biol Macromol 2018;117:418–26.
[111] Huang HY, Hu SH, Chian CS, Chen SY, Lai HY, Chen YY. Self-assembling pva-f127 thermosensitive nanocarriers with highly sensitive magnetically-triggered drug release for epilepsy therapy in vivo. J Mater Chem 2012;22:8566–73.
[112] Rovers SA, Hoogenboom R, Kemmere MF, Keurentjes JTF. Repetitive on-demand drug release by magnetic heating of iron oxide containing polymeric implants. Soft Matter 2012;8:1623–7.
[113] Kim DH, Vitol EA, Liu J, Balasubramanian S, Gosztola DJ, Cohen EE, et al. Stimuli-responsive magnetic nanomicelles as multifunctional heat and cargo delivery vehicles. Langmuir 2013;29:7425–32.
[114] Hayashi K, Nakamura M, Miki H, Ozaki S, Abe M, Matsumoto T, et al. Magnetically responsive smart nanoparticles for cancer treatment with a combination of magnetic hyperthermia and remote-control drug release. Theranostics 2014;4:834–44.
[115] Jaiswal MK, De M, Chou SS, Vasavada S, Bleher R, Prasad PV, et al. Thermoresponsive magnetic hydrogels as theranostic nanoconstructs. ACS Appl Mater Interfaces 2014;6:6237–47.
[116] Wang H, Yi J, Mukherjee S, Banerjee P, Zhou S. Magnetic/NIR-thermally responsive hybrid nanogels for optical temperature sensing, tumor cell imaging and triggered drug release. Nanoscale 2014;6:13001–11.
[117] Kulshrestha P, Gogoi M, Bahadur D, Banerjee R. In vitro application of paclitaxel loaded magnetoliposomes for combined chemotherapy and hyperthermia. Colloids Surf B 2012;96:1–7.
[118] Mengesha AE, Wydra RJ, Hilt JZ, Bummer PM. Binary blend of glyceryl monooleate and glyceryl monostearate for magnetically induced thermo-responsive local drug delivery system. Pharm Res 2013;30:3214–24.
[119] Bannwarth MB, Ebert S, Lauck M, Ziener U, Tomcin S, Jakob G, et al. Tailor-made nanocontainers for combined magnetic-field-induced release and MRI. Macromol Biosci 2014;14:1205–14.
[120] Qu Y, Li J, Ren J, Leng J, Lin C, Shi D. Enhanced synergism of thermo-chemotherapy by combining highly efficient magnetic hyperthermia with magnetothermally-facilitated drug release. Nanoscale 2014;6:12408–13.
[121] Louguet S, Rousseau B, Epherre R, Guidolin N, Goglio G, Mornet S, et al. Thermoresponsive polymer brush-functionalized magnetic manganite nanoparticles for remotely triggered drug release. Polym Chem 2012;3:1408–17.
[122] Chiang WL, Ke CJ, Liao ZX, Chen SY, Chen FR, Tsai CY, et al. Pulsatile drug release from plga hollow microspheres by controlling the permeability of their walls with a magnetic field. Small 2012;8:3584–8.
[123] Hu X, Wang Y, Zhang L, Xu M, Zhang J, Dong W. Magnetic field-driven drug release from modified iron oxide-integrated polysaccharide hydrogel. Int J Biol Macromol 2018;108:558–67.
[124] Hu SH, Liao BJ, Chiang CS, Chen PJ, Chen IW, Chen SY. Core-shell nanocapsules stabilized by single-component polymer and nanoparticles for magneto-chemotherapy/hyperthermia with multiple drugs. Adv Mater 2012;24:3627–32.
[125] Zheng C, Ding Y, Liu X, Wu Y, Ge L. Highly magneto-responsive multilayer microcapsules for controlled release of insulin. Int J Pharmaceut 2014;475:17–24.
[126] Oliveira H, Pérez-Andrés E, Thevenot J, Sandre O, Berra E, Lecommandoux S. Magnetic field triggered drug release from polymersomes for cancer therapeutics. J Control Release 2013;169:165–70.
[127] CazaresCortes E, Espinosa A, Guigner JM, Michel A, Griffete N, Wilhelm C, et al. Doxorubicin intracellular remote release from biocompatible oligo (ethylene glycol) methyl ether methacrylate-based magnetic nanogels triggered by magnetic hyperthermia. ACS Appl Mater Interfaces 2017;9:25775–88.
[128] Perera AS, Zhang S, Homer-Vanniasinkam S, Coppens MO, Edirisinghe M. Polymer-magnetic composite fibers for remote-controlled drug release. ACS Appl Mater Interfaces 2018;10:15524–31.
[129] Gao Y, Chang MW, Ahmad Z, Li JS. Magnetic-responsive microparticles with customized porosity for drug delivery. RSC Adv 2016;6:88157–67.
[130] Yan Q, Yuan J, Cai Z, Xin Y, Kang Y, Yin Y. Voltage-responsive vesicles based on orthogonal assembly of two homopolymers. J Am Chem Soc 2010;132:9268–70.
[131] Qu J, Zhao X, Ma PX, Guo B. Injectable antibacterial conductive hydrogels with dual response to an electric field and ph for localized "smart" drug release. Acta Biomater 2018;72:55–69.
[132] Liu S, Fu Y, Li G, Li L, HKw Law, Chen X, et al. Conjugated polymer for voltage-controlled release of molecules. Adv Mater 2017;29(1701733): 1–8.
[133] Kolosnjaj-Tabi J, Gibot L, Fourquaux I, Golzio M, Rols MP. Electric field-responsive nanoparticles and electric fields: physical, chemical, biological mechanisms and therapeutic prospects. Adv Drug Deliv Rev 2019;138:56–67.
[134] George PM, LaVan DA, Burdick JA, Chen CY, Liang E, Langer R. Electrically controlled drug delivery from biotin-doped conductive polypyrrole. Adv Mater 2006;18:577–81.
[135] Saigal R, Cimetta E, Tandon N, Zhou J, Langer R, Young M, et al. Electrical stimulation via a biocompatible conductive polymer directs retinal progenitor cell differentiation. 2013 35th Ann Int Confer IEEE Eng Med Biol Soc 2013:1627–31.
[136] Ge J, Neofytou E, Cahill IIITJ, Beygui RE, Zare RN. Drug release from electric-field-responsive nanoparticles. ACS Nano 2011;6:227–33.
[137] Mura S, Nicolas J, Couvreur P. Stimuli-responsive nanocarriers for drug delivery. Nat Mater 2013;12:991–1003.
[138] Chang X, Cheng Z, Ren B, Dong R, Peng J, Fu S, et al. Voltage-responsive reversible self-assembly and controlled drug release of ferrocene-containing polymeric superamphiphiles. Soft Matter 2015;11:7494–501.
[139] Kim JA, Kim JC. Temperature and electric field-triggerable liposomes incorporating poly (hydroxyethyl acrylate-co-hexadecyl acrylate-co-carboxyethyl acrylate). J Ind Eng Chem 2018;62:383–91.
[140] Liu HW, Hu SH, Chen YW, Chen SY. Characterization and drug release behavior of highly responsive chip-like electrically modulated reduced graphene oxide-poly (vinyl alcohol) membranes. J Mater Chem 2012;22:17311–20.
[141] Servant A, Methven L, Williams RP, Kostarelos K. Electroresponsive polymer-carbon nanotube hydrogel hybrids for pulsatile drug delivery in vivo. Adv Healthc Mater 2013;2:806–11.
[142] Servant A, Leon V, Jasim D, Methven L, Limousin P, Fernandez-Pacheco EV, et al. Graphene-based electroresponsive scaffolds as polymeric implants for on-demand drug delivery. Adv Healthc Mater 2014;3:1334–43.
[143] Chen W, Du J. Ultrasound and pH dually responsive polymer vesicles for anticancer drug delivery. Sci Rep 2013;3(2162):1–9.
[144] Lee JY, Carugo D, Crake C, Owen J, de Saint Victor M, Seth A, et al. Nanoparticle-loaded protein-polymer nanodroplets for improved stability and conversion efficiency in ultrasound imaging and drug delivery. Adv Mater 2015;27:5484–92.
[145] Liu R, Tang J, Xu Y, Dai Z. Bioluminescence imaging of inflammation in vivo based on bioluminescence and fluorescence resonance energy transfer using nanobubble ultrasound contrast agent. ACS Nano 2019;13:5124–32.
[146] Lin PL, Eckersley RJ, Hall EAH. Ultrabubble: a laminated ultrasound contrast agent with narrow size range. Adv Mater 2009;21:3949–52.
[147] Chen Y, Yin Q, Ji X, Zhang S, Chen H, Zheng Y, et al. Manganese oxide-based multifunctionalized mesoporous silica nanoparticles for pH-responsive MRI, ultrasonography and circumvention of MDR in cancer cells. Biomaterials 2012;33:7126–37.
[148] Schutt EG, Klein DH, Mattrey RM, Riess JG. Injectable microbubbles as contrast agents for diagnostic ultrasound imaging: the key role of perfluorochemicals. Angew Chem Int Ed Engl 2003;42:3218–35.
[149] Qian X, Wang W, Kong W, Chen Y. Organic-inorganic hybrid hollow mesoporous organosilica nanoparticles for efficient ultrasound-based imaging and controlled drug release. J Nanomater 2014;2014:1–8.
[150] Bozhko D, Osborn EA, Rosenthal A, Verjans JW, Hara T, Kellnberger S, et al. Quantitative intravascular biological fluorescence-ultrasound imaging of coronary and peripheral arteries in vivo. Eur Heart J Card Im 2017;18:1253–61.
[151] Bosca F, Bielecki PA, Exner AA, Barge A. Porphyrin-loaded pluronic nanobubbles: a new us-activated agent for future theranostic applications. Bioconjug Chem 2018;29:234–40.
[152] Wilson K, Homan K, Emelianov S. Biomedical photoacoustics beyond thermal expansion using triggered nanodroplet vaporization for contrast-enhanced imaging. Nat Commun 2012;3(618):1–10.
[153] Liu J, Detrembleur C, Mornet S, Jerome C, Duguet E. Design of hybrid nanovehicles for remotely triggered drug release: an overview. J Mater Chem B 2015;3:6117–47.
[154] Wu P, Jia Y, Qu F, Sun Y, Wang P, Zhang K, et al. Ultrasound-responsive polymeric micelles for sonoporation-assisted site-specific therapeutic action. ACS Appl Mater Interfaces 2017;9:25706–16.
[155] Zheng S, Jin Z, Han J, Cho S, Ko SY, Park JO, et al. Preparation of hifu-triggered tumor-targeted hyaluronic acid micelles for controlled drug release and enhanced cellular uptake. Colloids Surf B 2016;143:27–36.
[156] Rizzitelli S, Giustetto P, Cutrin JC, Castelli DD, Boffa C, Ruzza M, et al. Sonosensitive theranostic liposomes for preclinical in vivo mri-guided visualization of doxorubicin release stimulated by pulsed low intensity non-focused ultrasound. J Control Release 2015;202:21–30.
[157] Airan RD, Meyer RA, Ellens NP, Rhodes KR, Farahani K, Pomper MG, et al. Noninvasive targeted transcranial neuromodulation via focused ultrasound gated drug release from nanoemulsions. Nano Lett 2017;17:652–9.
[158] Lee JY, Carugo D, Crake C, Owen J, de Saint Victor M, Seth A, et al. Nanoparticle-loaded protein-polymer nanodroplets for improved stability and conversion efficiency in ultrasound imaging and drug delivery. Adv Mater 2015;27:5484–92.

[159] Paris JL, Cabañas MV, Manzano M, Vallet-Regí M. Polymer-grafted mesoporous silica nanoparticles as ultrasound-responsive drug carriers. ACS Nano 2015;9:11023–33.
[160] Huang J, Li W, Li Y, Luo C, Zeng Y, Xu Y, et al. Generation of uniform polymer eccentric and core-centered hollow microcapsules for ultrasound-regulated drug release. J Mater Chem B 2014;2:6848–54.
[161] Ninomiya K, Yamashita T, Kawabata S, Shimizu N. Targeted and ultrasound-triggered drug delivery using liposomes co-modified with cancer cell-targeting aptamers and a thermosensitive polymer. Ultrason Sonochem 2014;21:1482–8.
[162] Hosseini-Nassab N, Samanta D, Abdolazimi Y, Annes JP, Zare RN. Electrically controlled release of insulin using polypyrrole nanoparticles. Nanoscale 2017;9:143–9.
[163] Deng Z, Guo Y, Zhao X, Ma PX, Guo B. Multifunctional stimuli-responsive hydrogels with self-healing, high conductivity, and rapid recovery through host-guest interactions. Chem Mater 2018;30:1729–42.